Temporal carbon assessment through radiometric and repeat measure analysis in a mangrove

Karen Lamont 43434010

Department of Environmental Sciences

Date of Final Submission: 13 December 2018

Statement of Originality

This work has not previously been submitted for a degree or diploma in any university. To the best of my knowledge and belief, the thesis contains no material previously published or written by another person except where due reference is made in the thesis itself.

(Signed):   Date: 13/12/2018

Karen Lamont

Table of Contents

i. List of Tables

ii. List of Figures

iii. Abstract

Mangrove ecosystems store large quantities of organic carbon for long periods of time. This study explores long-term 'blue carbon' stock change through the first comparative study of radiometric analysis and repeat measures over a multi-decadal period in a mangrove system. Examining a tall and stunted forest, radiometric analysis estimated a soil organic carbon accumulation rate of 4.3 ± 1 Mg C ha^{-1} y^{-1} in the tall gallery forest and 1.7 ± 0 Mg C ha^{-1} y^{-1} in a stunted mangrove encroachment zone. Repeat measures of only root carbon estimated 5.06 Mg C ha^{-1} y^{-1} in the tall forest and 6.63 Mg C ha^{-1} y^{-1} in the stunted forest – suggesting an underestimate by radiometric dating of 15% and 74% in the tall and stunted forest respectively. Past bulk carbon measures were not available, however it is likely this discrepancy would be higher if informed by repeat measures of bulk carbon. A higher carbon stock in the stunted forest was attributed to root mass increase, associated with landward mangrove encroachment. Extrapolated to the entire region of NSW, we estimate that mangrove encroachment has contributed at least ~1,853,000 Mg C sequestration over the 70 years for which this has been observed in NSW.

1. Introduction

1.1 Blue carbon

'Blue carbon' refers to carbon that is stored in coastal ecosystems, specifically mangroves, salt marsh and seagrass. Carbon accumulates in aboveground biomass, but most is stored in living and non-living biomass belowground, as a result of preservation induced by tidal inundation. This burial of carbon in soils and sediments creates some of the oldest and largest carbon sinks in the world (Grimsditch et al., 2013; Howard et al., 2014; Mcleod et al., 2011). Coastal ecosystems therefore play a potentially important role in carbon cycling and climate change mitigation, as they possess a natural mechanism of sequestering carbon over time (Bouillon et al., 2008; Chmura et al., 2003; Duarte et al., 2005). Despite their evident importance, coastal ecosystems are currently facing extensive loss, attributable to the threat of sea level rise, as well as land use conversion for agricultural, industrial and urban development (Lovelock et al., 2015; Rogers et al., 2016; Webb et al., 2013). It is therefore imperative to improve our understanding of how tidal carbon sinks naturally change over time, and how they will respond to climate change and human pressure.

Blue carbon habitats are generally more efficient than terrestrial ecosystems at sequestering and storing large quantities of carbon. Waterlogged soils suppresses the oxidation and remineralisation of carbon, and thereby suppressing release of CO_2 into the atmosphere (Chmura, 2013; Howard et al., 2014; Mcleod et al., 2011; see Figure 1). Tidal wetlands generally have low CH_4 emissions as sulfates from tidal flows encourage the dominance of sulfur-reducing archaea and the anaerobic oxidation of methane (Howe et al., 2009; Saintilan et al., 2013), furthering these ecosystem's efficiency of mitigating greenhouse gas emissions. The provenance of carbon is a significant question, as it can originate autochthonously and allochthonously. Autochthonous carbon is produced and deposited *in situ*. Allochthonous carbon is produced elsewhere, transported and then deposited in blue carbon ecosystems, adding to the carbon sink (Howard et al., 2014; Kristensen et al., 2008; see Figure 1). Permanence refers to how

long the carbon will remain deposited within the ecosystem. It is important to consider these concepts when examining long-term, decadal change in carbon sinks as provenance and permanence influences the reliability of a sink's potential to store carbon over long periods of time, and ultimately determine whether or not a sink is financially worth investing in.
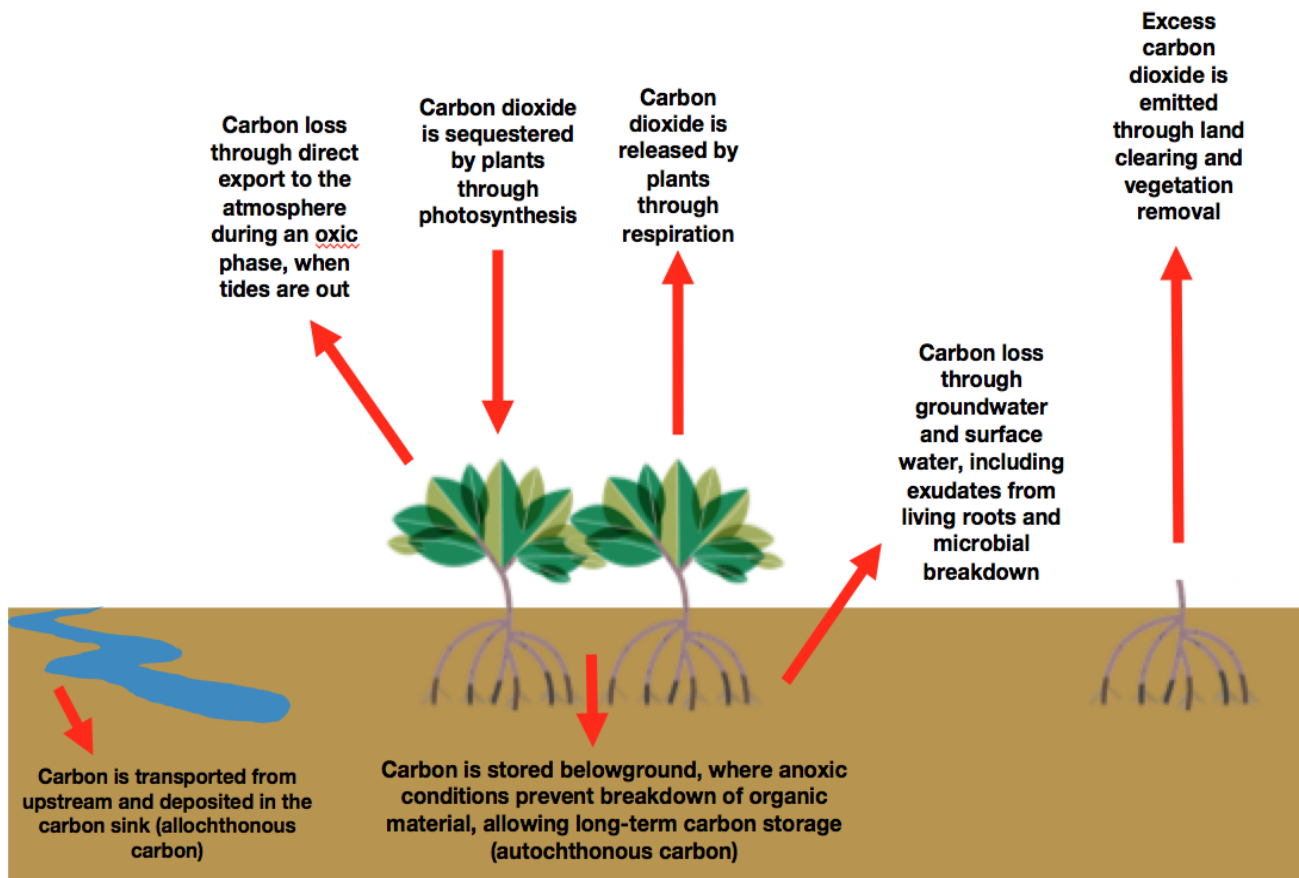
Figure 1: Visual diagram of how coastal ecosystems capture and release carbon.

1.2 Importance of studying blue carbon sinks

Coastal ecosystems are generally more efficient at sequestering carbon than terrestrial ecosystems, making them a significant priority for climate mitigation schemes. Figure 2 shows the potential of tidal wetlands, including mangroves, salt marsh and seagrass, and the higher rates of carbon burial compared to terrestrial forests.

More importantly, if these ecosystems are disturbed or cleared, substantial quantities of CO_2 might be released back into the atmosphere, which would contribute to radiative forcing (Donato et al., 2011; Pendleton et al., 2012). Blue carbon sinks are susceptible to shifting from stores of carbon to sources of carbon in response to land-use changes, reiterating the necessity to better develop our understanding of how carbon sinks change with time (Mcleod et al., 2011). Table 1 demonstrates how large these quantities of CO_2 emissions may be.
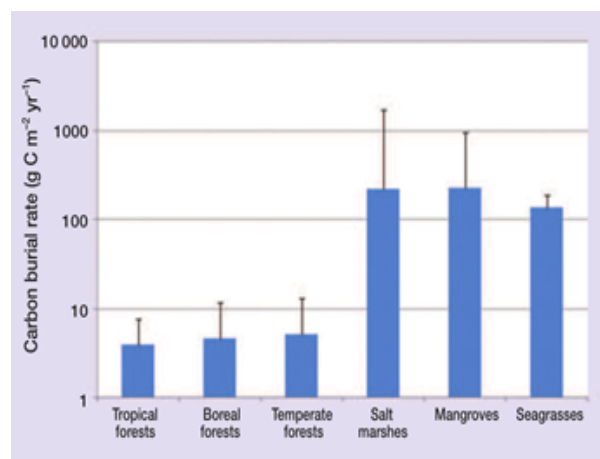
Figure 2: Graph of mean long-term rates of carbon burial, comparing terrestrial ecosystems and vegetated coastal ecosystems (From Mcleod et al., 2011, *Front. Ecol. Environ.* p. 556)

Table 1: Estimates of how much CO_2 is released into the atmosphere as a result of land-use change in coastal ecosystems, and estimated economic costs of emission (From Pendleton et al., 2012, *PLos One*, p. 3).

Ecosystem	Global extent (Mha)	Current conversion rate (% yr^{-1})	Near-surface carbon susceptible (top meter sediment+biomass, Mg CO_2 ha^{-1})	Carbon emissions (Pg CO_2 yr^{-1})	Economic cost (Billion US$ yr^{-1})
Tidal Marsh	2.2–40 (5.1)	1.0–2.0 (1.5)	237–949 (593)	**0.02–0.24 (0.06)**	**0.64–9.7 (2.6)**
Mangroves	13.8–15.2 (14.5)	0.7–3.0 (1.9)	373–1492 (933)	**0.09–0.45 (0.24)**	**3.6–18.5 (9.8)**
Seagrass	17.7–60 (30)	0.4–2.6 (1.5)	131–522 (326)	**0.05–0.33 (0.15)**	**1.9–13.7 (6.1)**
Total	33.7–115.2 (48.9)			**0.15–1.02 (0.45)**	**6.1–41.9 (18.5)**

Furthermore, tidal wetlands offer a multitude of ecosystem services including storm surge protection, sediment trapping, nutrient recycling, erosion prevention, coastal habitats for marine species, a food source for coastal communities, in addition to carbon sequestration (Howard et al., 2014). If preserved for carbon storage, tidal wetlands could simultaneously be utilised for a variety of sustainable development opportunities, all of which would contribute to local and international efforts of minimising human impact upon the environment.

1.3 Study aims

Long-term carbon preservation is an integral part of carbon cycling and mitigation and could play an important role in offsetting large quantities of greenhouse gas emissions. Increasingly, investors in the carbon market are seeking projects that can provide strong evidence of long-term additions to the carbon store, and the degree of certainty in the measurement of additional carbon sequestration directly influences the carbon price (Marland et al., 2001). Despite this, few carbon sequestration projects in tidal wetlands are of sufficient duration to allow for a meaningful time-series of carbon store change detection (Thomas, 2014). This thesis will assess the temporal dynamics of carbon storage and accumulation across a 30-year timeframe, utilising a unique set of measures taken within the study site in the late 1980's. The specific objectives are to:

1. Quantify carbon stock gain over a 30-year period by comparing historic data on above and blelowground mangrove biomass (Saintilan 1989;1995) with present-day estimates using the same techniques at the same sites.
2. Quantify carbon accumulation rates since 1989 to determine temporal changes over a 30-year period.
3. Determine what variables have influenced carbon stores and fluxes over a 30-year period.
4. Quantify and compare the autochthonous and allochthonous input to carbon accumulation over the time period.
5. Validate the repeat measure method by comparing the insights gained to alternative methods of long-term, temporal analysis in the literature.

2. Literature review

Coastal ecosystems, including mangrove forests, have been identified as a significant priority for climate action schemes in the literature, due to their potential to capture large quantities of atmospheric carbon for extensive periods of time. This brief review of the literature will summarise estimates of the global store of carbon in coastal wetlands,

environmental factors contributing to variability in space and time, and finishing with a review of methods for the estimation of store and accumulation.

2.1 Estimating global blue carbon stocks

The earliest development in quantifying global blue carbon stocks is recorded by Twilley et al., (1992), who synthesised local data sets of above and belowground biomass to come to an estimate of 4.03 Pg C in global mangrove stocks. No report of soil depth was recorded. Following Twilley et al., (1992), Chmura et al., (2003) published a review on global soil carbon stocks in mangrove and salt marsh at depths of 0-50cm. Globally, salt marsh carbon stock was estimated to be 0.43±0.03 Pg C and mangrove carbon stock was estimated to be 0.5±0.4 Pg C. At the time, soil carbon store estimates were standardised to a depth range of 0-100cm, however this was argued to be potentially underestimating total belowground carbon stocks, a point which has been further expanded in more recent literature (Atwood et al., 2017). Accounting for variability in depth, the overall magnitude of global carbon storage in coastal wetlands was estimated to be approximately ≥10 Pg C, however it was acknowledged that further data would be needed to verify this (Chmura et al., 2003). A key revision came from Donato et al., (2011), who used field measurements to determine global carbon stock of mangroves in the Indo-Pacific region, an area that had previously been poorly studied. Donato et al., (2011) assessed whole-ecosystem carbon storage (incorporating tree and dead wood biomass, and soil carbon stock ranging to depths of 50-300cm) for Indo-Pacific mangroves. They estimated a mean ecosystem stock of 1023 Mg C ha-1^{-1} for Indo-Pacific mangroves, of which they extrapolated to a global stock of 4-20 Pg C. Duarte et al., (2013) estimated a global soil carbon stock in mangroves, salt marsh and seagrasses of 19.65 Pg C to depths of 0-100cm, which is consistent with Donato et al., (2011)'s estimate of 4-20 Pg C, and builds upon Twilley et al., (1992) and Chmura et al., (2003). Jardine and Siikamäki, (2014) estimated a global soil mangrove carbon stock of 5.0±0.9 Pg C, which is closer to Chmura et al., (2003)'s estimate, however is still consistent with Donato et al. (2011)'s 4-20 Pg C. More recently, Rovai et al., (2018) estimated a global soil mangrove carbon stock of 2.26 Pg C, and Atwood et al., (2017)

estimated a global soil mangrove carbon stock of 2.6 Pg C, lower than the 4-20 Pg C
Donato et al., (2011) estimated.

Building on estimates from Southeast Asia, Alongi, (2012) estimated whole-ecosystem
(above and belowground, roots and wood production) mangrove carbon stock of the
Indo-Pacific to be 927 Mg C ha-1^{-1} using cores ranging from 62cm-400cm, and Liu et al.,
(2014) estimated above and belowground mangrove carbon stock of China to be
355.35±82.19 Mg C ha-1^{-1} to depths of 100cm. Alongi et al., (2016) refined previous
estimates of Indonesia, and re-estimated that the whole-ecosystem national seagrass
and mangrove stock is 3.4 Pg C at depths of 100cm, approximately 17% of the global
blue carbon stock. It is recognised that there is a comparable lack of data in Latin
American, South American and African regions (Alongi, 2012; Duarte et al., 2013).
Some studies have emerged, where Kauffman et al., (2014) estimated above and
belowground carbon stocks in the Dominican Republic to range from 706-1131 Mg C
ha-1^{-1} at depths of 0-100cm, and Kirui et al., (2013) mapped mangrove areal extent with
Landsat imagery along the coastline of Kenya. However, no regional carbon stock has
been estimated from this data. More refinement will be needed in these areas to fill
these gaps.

2.2 Variables that influence temporal change

2.2.1 Environmental setting

Twilley et al., (1992) reported that the proportional contribution of sinks differed
depending on latitude. Of the 4.03 Pg C global stock, 70% was estimated to occur in the
0° to 10° zone due to high discharge of major rivers. This increases the amount of
sediment and organic carbon transported and deposited into coastal wetlands,
demonstrating how hydrological variability can have an impact on carbon sink dynamics.
Chmura et al., (2003) found that temperature could impact carbon stocks, indicating that
as temperature increases, carbon density decreases. This is most likely attributable to
faster rates of microbial decay and decomposition, leading to release of CO_2. With the

slow increase of annual average temperature due to climate change, carbon stocks may begin to emit CO_2 faster over long time frames. However, it is also recognised that the increased productivity from higher temperatures may act as a counter-balance to increased decomposition (Ouyang and Lee, 2014). A further key development is Saintilan et al., (2013), who found that greater tidal range will increase rates of vertical accretion. Without adequate frequency, depth and duration of tidal inundation, the capacity of tidal wetlands to
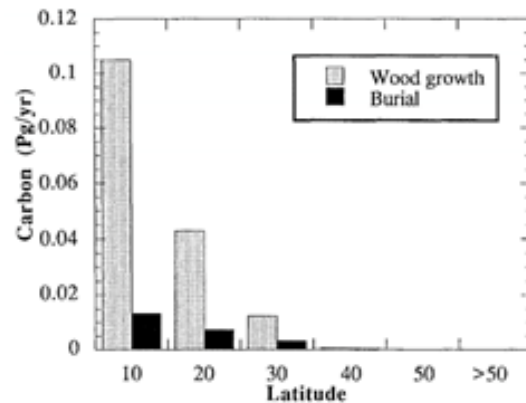
Figure 3: Above graph shows carbon burial rates in Pg y[-1] relative to latitudinal location, where carbon buried in sediment is black and carbon stored in wood is grey. 0° to 10° latitudes show the highest carbon stocks (From Twilley et al., 1992, *Wat. Air. Soil. Poll.* p. 272)

vertically accrete - through organic production and/or mineral deposition - may be impeded, along with their capacity for blue carbon storage. Hydrogeomorphic setting is a further contributor, where sinks will store carbon more efficiently over time if they are situated in mesotidal and fluvial settings, in comparison to marine settings (Saintilan et al., 2013). Should any of these environmental factors change over time within a coastal ecosystem, blue carbon stocks are likely to also respond with change.

2.2.2 Vegetation

Choi et al., (2001) used radiometric dating to determine the age of carbon stocks in salt marshes. The results indicate that carbon content is highest in low marsh (the oldest area), and lowest in high marsh (the youngest area). Choi et al., (2001) interprets this in the context of rising sea levels, where salt marsh is evolving from high marsh to low marsh and expanding landward in response to sea level rise. This suggests that carbon stocks can increase over time due to sea level rise, if the ecosystem can keep pace, as landward expansion will create a larger surface area for salt marsh to store carbon. Thus, geomorphic changes and associated shifts in vegetation may be strong contributors to carbon stock change over time. This is furthered by Kelleway et al., (2016a), where the encroachment of mangroves into salt marsh over a 70-year period
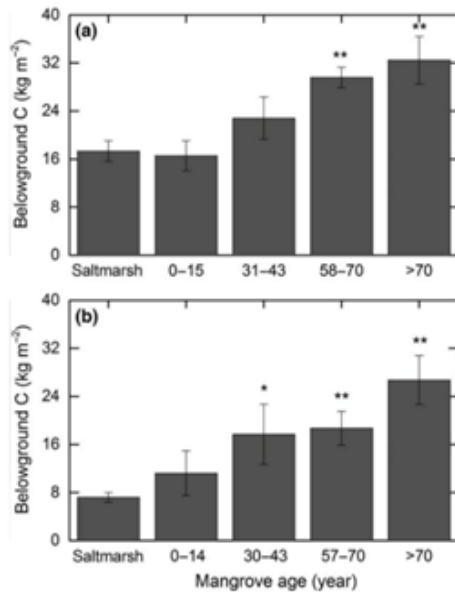
Figure 4: Belowground biomass estimates in kg m^{-2}, relative to ecosystem age, where (a) is a fluvial site and (b) is a marine site. Increasing trend can be seen as mangroves begin to encroach into salt marsh, where (a) has higher aboveground biomass (From Kelleway et al., 2016a, *Glo. Cha. Bio.* p. 1103)

was estimated to result in belowground carbon stocks by up to 500,865 Mg across the state of New South Wales. As mangroves continue to encroach further, it is likely that carbon stocks in Australia will increase with it.

Vegetation type is also an important contributor to variation in carbon stocks and fluxes. Lovelock et al., (2013) discovered that *Juncus kraussii* had a much higher rate of accumulation in comparison to *Sarcocornia quinqueflora*, (see Table 2). Lovelock et al., (2013) attributes this to *Juncus* rhizomes facilitating root and shoot development, which sequesters larger quantities of carbon. This conforms with the findings of Saintilan et al., (2013), who also found that *Juncus* had a much higher carbon stock compared to *Sarcocornia*, as well as *Sporobolous virginicus.* On the basis of stable isotope signatures, they argue that autochthonous plant material plays a strong role in belowground carbon, as the root material contributes significantly to soil carbon stock. Lovelock et al., (2013) also considers vertical accretion and elevation change to be factors influencing spatial variation in stocks (see Table 2).

Jennerjahn and Ittekkot, (2002) found that leaves are a major source of carbon that accumulates in mangrove sediments, attributing abundant litterfall to high levels of carbon sequestration. Saintilan et al. (2013) also discusses the importance of litter fall, specifically the grey mangrove *Avicennia marina*, though find the relative importance of leaf material to carbon stocks decreases with time (i.e., down profile). Trevathan-Tackett et al., (2015) has found that allochthonous plant material might play a significant role in long-term carbon sequestration, including macroalgae (see Table 2). Thus, not

only does autochthonous vegetation appear to make a strong impact on carbon sinks, allochthonous material may also hold value to long-term blue carbon sequestration.

2.2.3 Sediment

Chmura et al. (2003) found that sediment deposition enhances carbon sequestration and concluded that variability in sediment accumulation rates is a major control of blue carbon storage, (see Table 2). Similarly, Lovelock et al., (2013) found that higher rates of vertical accretion and a moderate pace of elevation increase will result in larger stocks of carbon. Saintilan et al., (2013) warns however, that surface carbon accumulation is driven by the allochthonous input of sediment and has very low residence time, which most likely does not contribute to

Figure 5: Visual representation of Saintilan et al., (2013), showing that surface carbon accumulation measured by feldspar markers are not reliable indicators of permanent carbon storage. Deeper coring with ^{210}Pb dating produces far more reliable results, as depicted. Surface carbon measurements should thus not be used as indicators for economic schemes or policy development. (Own figure, concept from Saintilan et al., 2013, *Est. Coa. She. Sci.*)

permanent carbon storage. Sediment type can also influence carbon stock change, where sites with silts and muds had a higher retention of carbon down-core, compared to areas with aerated sandy substrates (Saintilan et al., 2013). Comparable results were reported by Kelleway et al., (2016b) who determined that high carbon stocks were associated with fine-grained, fluvial sediments, and that sediment size can be used as a predictor for carbon density. Twilley et al., (2018) and Rovai et al. (2018) further build on this and argue that carbonate settings have been significantly underestimated in the literature, and further assessment in categorising specific environmental settings of blue carbon stocks are required. Thus, sedimentary changes over time can also cause significant temporal change in blue carbon stocks.

Table 2: Summary of key literature explaining variables that influence carbon stock change temporally. C = Carbon.

Year	Paper	Variable	Impact
1992	Twilley et al.	- Hydrology - Latitude - Climate	- Higher discharge in latitudinal location due to higher precipitation levels - More sediment transport = higher C stock
2002	Choi et al.	- SLR - Vegetation	- SLR encourages landward expansion - Vegetation changes to move inland, more surface area, higher C stock
2002	Jennerjahn and Ittekot	- Vegetation	- Litter fall is strong contributor to higher C stocks
2003	Chmura et al.	- Climate - Sediment - Vegetation	- Higher temp = lower C stock, as a result of faster microbial decay - Higher sediment rate = more trapping of organic matter from vegetation growing on the soil surface, such as macrophytes and microflora = higher C stock
2013	Saintilan et al.	- Geomorphic setting - Vegetation - Sediment	- Frequent tidal inundation increases C stock - Mesotidal and fluvial settings better than marine setting - *Juncus* stores C at fastest rate - Silts and muds store C better than sandy sediment - Allochthonous input does not contribute to permanent C store
2013	Lovelock et al.	- Vegetation - Sediment	- *Juncus* stores C better than *Sarcocornia* and *Sporobolous* - Mean for *Juncus* was 0.76 ± 0.16 Mg C ha-1^{-1} y^{-1} - Mean for *Sarcocornia* was 0.086 ± 0.04 Mg C ha-1^{-1} y^{-1} - Higher rate of vertical accretion = higher C stock - Moderate elevation helps C stock build over time
2015	Trevathan-Tackett et al.	- Vegetation	- Marine macrophytes could play strong role in C stock - high rates of production, fragmentation and capacity to be transported easily
2016a	Kelleway et al.	- Vegetation	- Encroachment of mangrove onto salt marsh results in higher C stock - Mangroves are more capable of sequestering C - Increased areal extent/surface area of tidal wetlands, particularly mangroves, will increase C stock

| 2016b | Kelleway et al. | - Sediment
- Geomorphic setting | - Fine-grained sediment is more capable of storing C
- Fine-grained fluvial sites had highest C density
- Suggests using sedimentary classification system to find blue carbon hot spots |

2.3 Rates of accumulation

To quantify the change that has occurred in blue carbon stocks over time, rates of carbon accumulation have been globally estimated to further enhance our understanding of how quickly carbon sinks can change within a temporal scale. All rates fall within a range of 0.01 Pg C y^{-1} to 0.167 Pg C y^{-1}. It is important to note that some studies did not include depth details, as they were based off the collation of multiple data sets or other measures. It may therefore be possible that these results may be underestimates, as there is no physical measure of data present.

Table 3: Summary of global rates of carbon accumulation in the literature. M = Mangrove, SM = Salt Marsh, S = Seagrass.

Year	Paper	Habitat	Depth	Estimate
1992	Twilley et al.	M	No record	0.02 Pg C y^{-1}
2002	Jennerjahn and Ittekkot	M	Based on litter fall	0.023 Pg C y^{-1}
2003	Chmura et al.	M, SM	0-50cm	0.0446 Pg C y^{-1}
2005	Duarte et al.	M, SM, S	No record	0.1114 Pg C y^{-1}
2011	Mcleod et al.	M, SM, S	No record	0.1585 Pg C y^{-1} ^
2012	Breithaupt et al.	M	No record	0.026 Pg C y^{-1}
2012	Alongi	M, SM, S	62-400cm	0.167 Pg C y^{-1}
2013	Duarte et al.	M, SM, S	0-100cm	0.14975 Pg C y^{-1} ^
2014	Ouyang and Lee	SM	47 cores <100cm, 3 cores >100cm	0.0102 Pg C y^{-1}

| 2014 | Alongi | M | No record | 0.024 Pg C y^{-1} |

2.4 Examining change in long-term decadal studies

Few studies have assessed changes in carbon sinks along decadal timelines. Three experimental approaches have been identified (Table 4), with most studies applying a synthesis of approaches to produce results.

Table 4: Experimental approaches used to assess temporal change in carbon sinks.

Experimental Approach	Method
Repeat measures	Taking initial measurements and taking replicate measurements after a certain period of time, usually a decadal scale
Space-for-time substitution	Using space as a substitute for time, and taking measurements in young and old sites to use as a comparison
Radiometric dating	Using a reconstructed sedimentary history through ^{210}Pb coring or carbon isotope tracing to recreate carbon stock change

2.4.1 Repeat measures

Lunstrum and Chen, (2014) examined the impact of mangrove afforestation in Southeast China with repeat measures annually at two afforested mangroves for six years from the time of planting. They also took measurements at 0, 6, 20 and 70 year old sites, along a 70-year chronosequence. In both the repeat measurements and chronosequence, carbon stock increased with forest age. Their repeat measures of belowground carbon consisted in 10cm cores, from which they demonstrated an increase in percent organic carbon over time. Overall, Lunstrum and Chen, (2014) demonstrate that restoration efforts have a positive impact on carbon accumulation rates, and that spatial variation in forest age has a significant influence on decadal scale changes in blue carbon sinks. A key result they found was that although the repeat measure results only span 6 years, these measures were less variable compared to the 70-year chronosequence. Repeat measure studies are scarce in the literature, with

Lunstrum and Chen, (2014) being one of the only assessments in long-term blue carbon studies to utilise this approach. This could be attributed to the time constraints of conducting replicate measurements and the inability to generate immediate results. This leaves a large gap in the literature that needs to be filled, as repeat measure studies can recreate an exact, precise timeline of changes in carbon dynamics over decadal scales, refining current understandings.

2.4.2 Space-for-time substitution

Osland et al., (2012) compared created tidal wetlands to natural mangrove wetlands in Florida over a 20-year chronosequence. Nine created tidal wetlands aged 2 to 20 years were compared to nine natural mangroves. They found that the initial herbaceous layer that was planted in the created wetlands, eventually transitioned into a mangrove forest within 13 years. This is attributed to adult mangrove development, which the herbaceous vegetation helped facilitate. Soil properties also underwent extreme changes. Initially, the soil had a very high sand content, low organic matter and very low carbon content. However, by the second decade, a peat layer began to develop in the upper 10cm, and by 20 years the soil properties were equivalent to soils in the 9 natural mangrove wetlands, (Figure 6). Osland et al., (2012) further argues that the rate of carbon accumulation will increase as mangrove forests mature, created and natural.
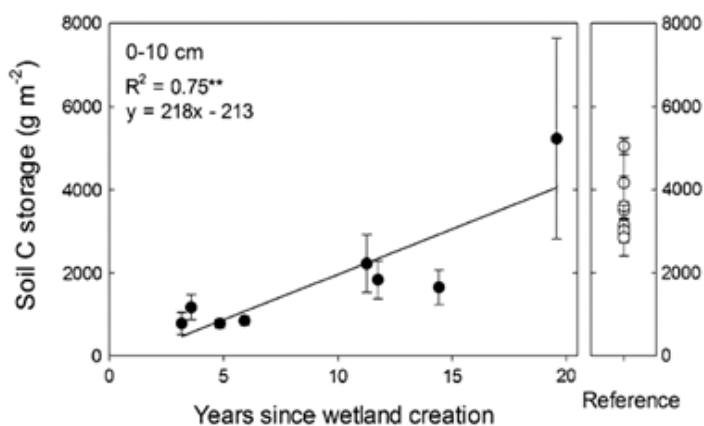
Figure 6: Soil carbon storage in g m^{-2} in created wetlands relative to age. As ecosystem age increases, soil carbon storage increases. Natural wetlands are used as a reference to the right, indicating by 20 years created wetlands are equivalent to natural conditions. (From Osland et al., 2012, *Eco.* p. 858)

Marchand, (2017) quantified soil carbon stock across a mudbank in French Guiana, along a chronosequence of 3 to 48 years. It was found that increasing forest age contributes to larger carbon stocks because it creates a pedogenetic layer that is enriched in autochthonous organic material over a long period of time, (Figure 7). The position in the tidal zone was also found to be important, particularly in this mudbank setting, as the low intertidal zone in this site has oxic and suboxic conditions, resulting in more oxidation and less carbon storage.

Figure 7: Correlation between organic carbon stock and mangrove age, where carbon stock increases as mangrove age increases in the pedogenetic layer. Senescent forests therefore have the highest carbon stock. (From Marchand, 2017, *For. Eco. Mng.* p. 97)
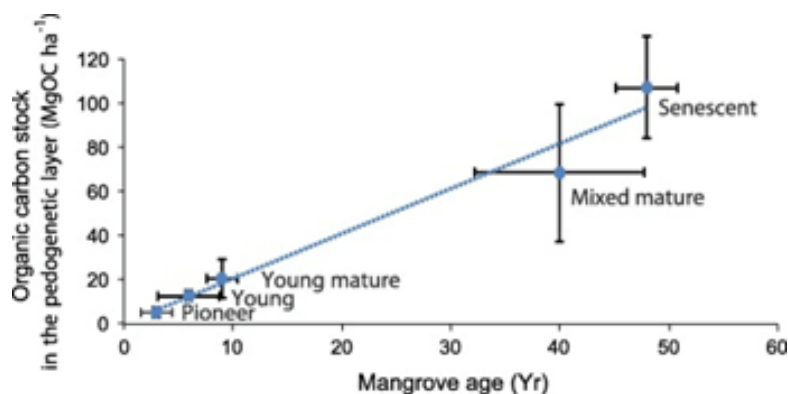
Both studies therefore reiterate that temporal dynamics can significantly influence carbon storage properties in tidal wetland ecosystems. Both ecosystems showed increased carbon stock with increased forest age. Osland et al., (2012) furthered the argument that vegetative restoration has a positive impact on carbon storage, and Marchand, (2017) further verified the significance of sediment and soil properties, and geomorphic setting. A more recent study in the area, Walcker et al., (2018), utilised a similar approach over a 66-year chronosequence and also found that soil carbon storage remains constant through time, despite plant carbon decreasing. The space-for-time approach is a commonly pursued experimental design in the literature and is a useful method of extrapolating long-term information without waiting the impractical length of time required to document long-term trends. However, this experimental design only ever gives an indication of what long-term change might be, and the potential for systematic bias in the location and characteristics of old and young sites precludes certainty in the reconstruction of temporal trends. Without direct repeat measures through time, we cannot accurately quantify how much carbon has accumulated in situ over time.

2.4.3 Radiometric dating

Radiometric dating has long been applied to reconstruct sedimentation chronologies, and by implication the rate of carbon accumulation in tidal wetland settings. For example, Kelleway et al., (2016a) assessed the continuous, lateral encroachment of mangroves into salt marsh in two Southeast Australian sites, one a mesohaline fluvial site and the other a marine embayment site, along a 70-year chronosequence. After 30 years a substantial increase in biomass was recorded, with higher results in the fluvial site, attributed to local factors including salinity, nutrient limitation and sedimentation. Using a ^{210}Pb core at a depth of 0-100cm, a reconstruction of the sedimentary history and carbon concentration was created, showing high carbon content from 0-25cm, which correlates with the development of a fine root-dominated peat layer following mangrove encroachment. Enhanced sedimentation is likely to

Figure 8: Down-core profile of ^{210}Pb core. Reconstruction of sedimentary history, where high carbon content is shown from 0-25cm (39±6 to 4±2 years), and peak in mass accumulation rate is shown at 30cm (71±8 years). (From Kelleway et al., 2016a, *Glo. Cha. Bio*. p. 1105)

have occurred prior to mangrove encroachment, and thus the peat layer development may explain the increase in carbon concentration as mangroves began to encroach salt marsh. Reiterating Osland et al., (2012), the development of a peat layer with simultaneous vegetation change plays a crucial role in decadal carbon sink change, and will likely continue to enrich carbon sinks over time. The combination of radiometric dating and space-for-time substitution has helped produce refined results, and is now a commonly pursued approach in the literature.

Many studies have emerged that utilise radiometric dating to reveal past changes in carbon dynamics as a means of future projection. Greiner et al., (2013) compared carbon accumulation rates in 10-year, 4-year and 0-year (bare sediment) old seagrasses, and found that the 10-year old seagrasses stored significantly more carbon at faster rates, as the more mature plants are able to stabilise and trap sediments more efficiently. Marbà et al., (2015) reiterates this, and found that continuously vegetated and re-vegetated seagrasses had significantly higher carbon stocks and faster rates of carbon accumulation, as opposed to areas where seagrass was cleared. Again, this is attributed to enhanced sediment trapping in vegetated areas, and emphasises the importance not only of vegetation, but of the benefits of re-vegetation and restorative management efforts in tidal wetlands.

Although radiometric dating is a valuable tool in temporal studies, the reliance on this method may be resulting in underestimations of carbon stocks in the literature. It is important to note that although radiometric dating can isolate specific points in time within belowground samples, it cannot reveal the age of the carbon - it will only reveal the approximate timing of the deposition of mineral material to the substrate. Thus, accumulation rates are based on sediment accumulation rather than carbon accumulation. Furthermore, it cannot determine how much biomass is developing and being introduced through time, as roots may grow both above and below dated sediment depths. Nor can it capture the rate of soil or biomass carbon decomposition. Additionally, due to significant expenses, this approach can often rely on the quality of small amounts of data, rather than large quantities of replicated data. Thus, similar to substituting space for time, there are limitations with solely using radiometric dating to quantify temporal change in carbon dynamics. Only repeat measures through time in the same space will accurately quantify carbon change.

2.5 Summary

The literature has shown that there is a likely correlation between vegetation, sediment and geomorphic setting, as these variables have been indicated to be key influences on

temporal change in carbon sinks. These variables are often interlinked, and have significant impact on instigating and maintaining long-term decadal scale changes. Results from restoration studies along chronosequences, as well as through radiometric dating, generally indicate that restorative management efforts have a positive impact on long-term carbon sink change and facilitate environments conducive of carbon preservation into the future. In terms of decadal studies, more revisions focusing on longer chronosequences need to be undertaken. Lunstrum and Chen, (2014) have completed the only repeat measure study in the literature, and produced an exact recreation of carbon stock change through time. This suggests that long-term research should be undertaken using repeat measures to generate more robust data and less variable results where possible. Furthermore, as outlined above, there are significant limitations in substituting space for time and utilising only radiometric dating. In the former, the comparison of old and young sites in temporal sequence might be confounded by bias in the location and character of these sites (younger sites might be in different geomorphic settings, for example, or subject to different nutrient regimes than those to which older sites were exposed). In the latter, the interpretation of carbon sequences with radiometric dating is confounded by contemporary root growth over a varity of depths. A combined experimental approach to long-term inter-decadal carbon accumulation would be ideal, in which repeat measures are used as the main source of comparison, but supplemented by radiometric techniques. The benchmark data of Saintilan (1989;1995) in which above and belowground biomass was measured on the Hawkesbury River, allows for just such an approach.

3. Study site

3.1 Spencer, Hawkesbury River, NSW

The study was conducted in a mangrove flat adjacent to the town of Spencer on the Hawkesbury River, New South Wales, (Figure 9), in order to replicate the above and belowground biomass estimate of Saintilan, (1989) and Saintilan, (1995). The Hawkesbury River estuary extends 120km from an entrance at Broken Bay to its tidal

limit at Richmond. Situated north of metropolitan Sydney, the Hawkesbury is one of the largest drowned estuarine valley environments in New South Wales (Saintilan, 1997; Saintilan and Hashimoto, 1999). It lies within a valley of Triassic quartz sandstone (Saintilan and Hashimoto, 1999), often called Hawkesbury sandstone, and consists of a freshwater zone, central brackish zone and marine zone (Saintilan, 1997). This allows for the growth of many estuarine ecosystems, including mangrove forests. Spencer itself is a small village on Wisemans Ferry Road, located on the northern bank of the Hawkesbury, close to confluence with Mangrove Creek (Boon, 2017). Two sites have been selected for analysis along a wide intertidal point bar in Spencer; a tall (~10.4m) *Avicennia marina* forest (S1), and a stunted (~2.1m) *Avicennia marina* and *Aegiceras corniculatum* mixed mangrove forest (S2), (Figure 9).
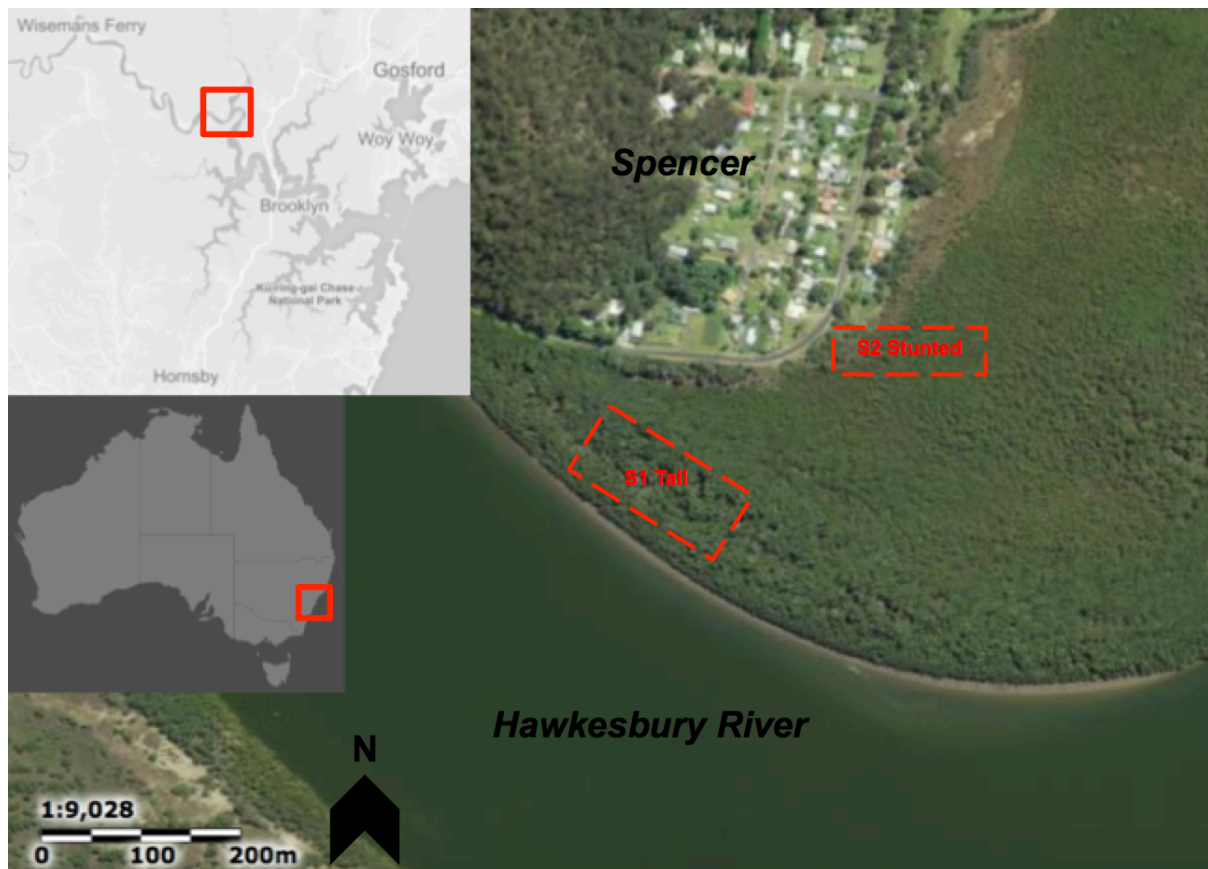
Figure 9: Map of study site at Spencer, Hawkesbury River, NSW.

Early aerial photography of the site shows that S1 accreted between 1947 (Caption A in Figure 10) and 1982. The survey of Saintilan (1989;1995) therefore represents a

maximum of 30 years of mangrove development, though represented at this time a tall forest of relatively high aboveground biomass.
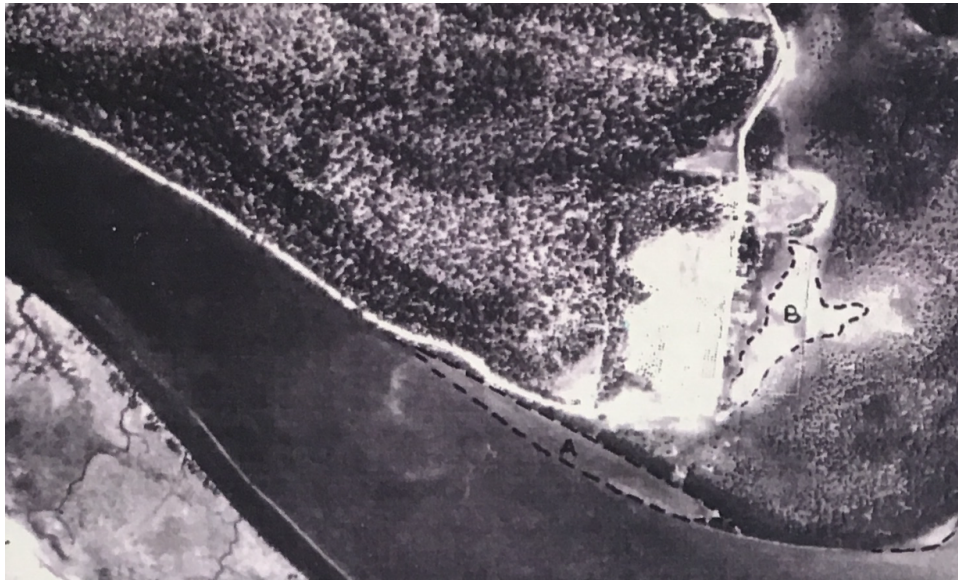
Figure 10: Historical aerial photograph of study sites in 1947, where A represents development of S1 and B represents development of S2 (Image from Saintilan, 1995, p. 35).

In 1947, S2 was an upper-intertidal mudflat, relatively free of mangrove and likely to have been dominated by saltmarsh (caption B in Figure 10). Aerial photography in following decades demonstrates a pattern of mangrove encroachment and thickening, and was one of the sites referenced by Saintilan and Williams, (1999) in making the case for a widespread regional trend of mangrove encroachment into saltmarsh.

Figure 11: Historical aerial photograph of study sites in 1982 (Image from Saintilan, 1995, p. 35).

Current aerial photography (2018, Figure 12), shows that S1 has developed into a dense forest, and S2 has become significantly more vegetated. These two sites were chosen for comparison with sampling conducted 30 years previously by Saintilan, (1989) allowing a contrast between a tall *A. marina* forest lower in the intertidal range, and a stunted mixed *A. marine/Aegiceras corniculatum* forest higher in the intertidal range, with both having established following the earliest photographs in 1945.

Installation of an HOBO water level sensor from 23 July 2018 to 22 August 2018 shows that S1 has higher frequencies of tidal inundation than S2, seen in Figure 13 below.

Figure 12: Historical aerial photograph of study sites in 2018 (From SIXMaps: https://maps.six.nsw.gov.au/).
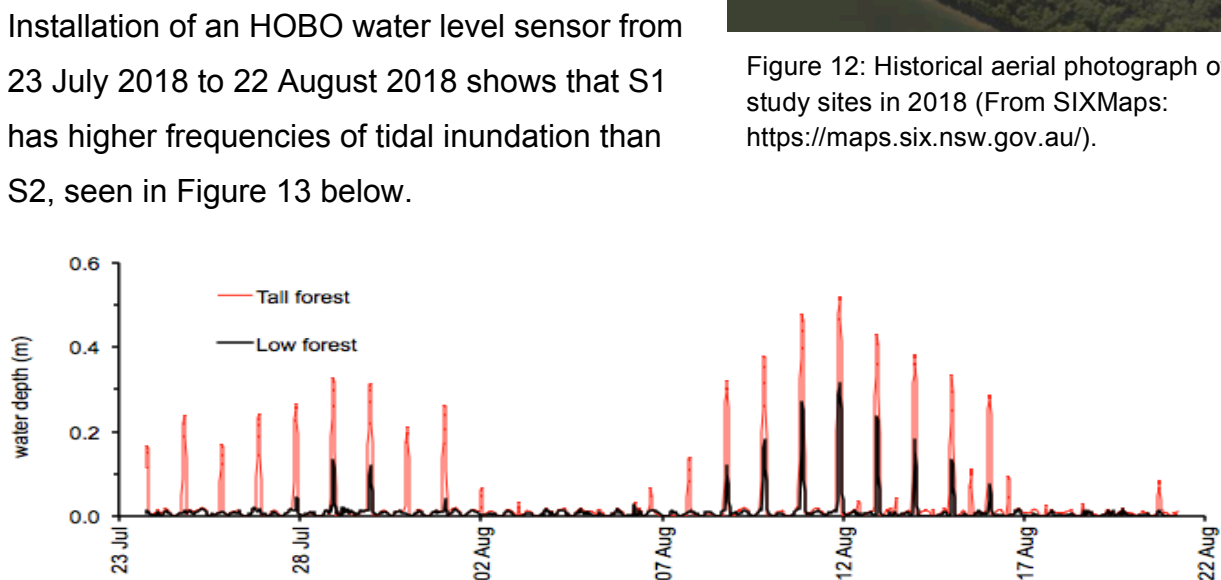
Figure 13: Tidal inundation data, July 2018 to August 2018, where red indicates S1 Tall and black indicates S2 Low/Stunted.

Our assumptions are that:

1. Both sites will show an accumulation in belowground root mass over time.
2. Both sites will show an accumulation in soil organic carbon over time.
3. The autochthonous production of mangrove root will be the dominant contributor to soil organic carbon accumulation over time.

20

4. Most root development in the past 30 years will have occurred above the 1989 horizon.

5. The upper intertidal site (S2) will have a lower rate of carbon accumulation given the lower inundation frequency, lower potential for plant growth and higher potential for soil oxidation.

4. Methods

Saintilan, (1989) and Saintilan, (1995) undertook an extensive survey of biomass characteristics along the Hawkesbury River during the late 1980's and early 1990's. Aboveground biomass measures of tall trees, dwarf trees, and shrubs, and belowground biomass measures of root mass were taken. Through the studies, Saintilan compiled a large dataset of biomass in Hawkesbury mangrove systems, that now dates back 3 decades. We repeated the measures Saintilan took 30 years ago in order to recreate a decadal timeline of carbon change within a mangrove ecosystem. Figure 14 shows below the logic of the comparative analysis that was undertaken to explore temporal carbon dynamics over a 30-year period in the Hawkesbury River.

2018 Sampling

1989 Sampling

Above-ground biomass 2018 (x')

Total C above 1989 surface in 2018

Above-ground biomass 1989 (x)

Root mass above 1989 surface in 2018 (y")

Root mass below 1989 surface in 1989 (y)

Root mass below 1989 surface in 2018 (y')

Total C below 1989 surface in 2018

30-yr above-ground sequestration $(a) = x' - x$

30-yr root mass accumulation $(b) = y'' + y' - y$

30-yr autochthonous accumulation $= a + b$

Figure 14: Visual representation of major components of site biomass being compared between the 1989 and 2018 surveys. Comparisons are made in 2018 between stocks above and below the 1989 horizon determined by radiometric analysis.

One impediment to the comparison is the absence of total soil organic matter measures from the Saintilan (1989;1995) surveys. However, the availability of above and belowground root mass data allows for a comparison of autochthonous carbon accumulation, both above and below the 1989 horizon identified through radiometric dating.

4.1 Aboveground biomass

Saintilan (1989;1995) calculated aboveground biomass through quadrats of 16m^2 in both S1 and S2, using standard tree measurements. For tall trees (>3m), height and diameter at breast height (DBH) were measured. For stunted trees, which included shrub trees (1.3-3m) and dwarf trees (<1.3m), a similar approach was used where height, DBH, diameter at 30cm (D30), diameter at 5cm (D5) and crown area was measured. To duplicate this, we measured 5 quadrats in each site. Quadrat sizes were modified to 100m^2 in S1 and 25m^2 in S2, to compensate for denser aboveground biomass since 1989. S1 quadrats were measured at 100m^2, as the tall trees were significantly sparser compared to the stunted trees, and a larger surface area was needed to capture variable data. S2 had smaller trees, but significantly denser vegetation, and thus only 25m^2 was needed. A total of 500m^2 was measured in S1 and a total of 125m^2 was measured in S2. A staff was used for height measurements less than 4 metres, and the mobile app 'Smart Measure' for measurements greater than 4 metres.

The data was applied to allometric equations supplied by Owers et al., (2018), (Table 5) to calculate aboveground biomass and carbon stock. The Owers et al., (2018) equations were selected as they were the most recent and accurate models in the literature to date. Initially, the original Saintilan, (1989;1995) equations were applied, however the calculations were largely over-estimated, and thus the revised Owers et al., (2018) equations were used instead. The Owers et al., (2018) equations were then also applied to the original Saintilan (1989;1995) data, to allow for comparison between surveys.

Table 5: Allometric equations applied to calculate aboveground biomass. Owers et al., (2018) was used to calculate final results, due to improved accuracy and reliability.

Paper	Allometric equation
Tall (>3m)	=(EXP(-3.84547+0.6216855*LN(Height*100)+1.2202155*LN(DBH)))*1.033
Shrub (1.3-3m)	=(EXP(-8.67075+1.5066493*LN(Height)+0.901411*LN(D30)+0.548275*LN(Crown Area)))*1.067
Dwarf (<1.3m)	=(EXP(-3.714181+0.6959132*LN(Height)+0.369786*LN(D5)+0.9578372*LN(Crown Area)))*1.046

4.2 Belowground carbon

Saintilan (1989;1995) calculated belowground biomass through pit excavation, where a shovel was used to excavate belowground material to a depth of 50cm (the point at which visible root material became scarce). This was repeated using the exact method, though the pit in each case was excavated to a greater depth allowing for surface accumulation since 1989. Soil organic carbon was sampled separately, using 100cm D-section cores, and these samples were subject to radiometric dating.

4.2.1 Belowground root mass and stable isotopes

Root material was excavated with a standard shovel, with dimensions of 15cm by 15cm, following the methods of Saintilan (1989;1995). Radiometric analysis (Figure 16) indicated that the contemporary surface was 12cm above the 1989 surface in S1 and 13cm above the 1989 surface in S2. Four samples were therefore taken at each site, at a depth of 12cm in S1 and 13cm in S2, in accordance with the 1989 horizon marker. Root material below the 1989 marker, to a depth of 62cm at S1 and S2, was also excavated. These depths took the total pit sample to the 50cm depth sampled by Saintilan (1989;1995). Samples were placed in cool storage and transported to the laboratory. Once returned to the laboratory, the samples were washed through a sieve to drain bulk sediment and collect all root biomass. The root material was then dried in the oven at 60°C for 72 hours. Samples were then weighed for their mass to compare to

Saintilan (1989;1995). Ten root sub-samples, five from each site, were prepared for stable isotope analysis to determine root %C and δ^{13}C by elemental analysis and IRMS respectively. Sub-samples were homogenised through the mortar and pestle approach and analysed at the Australian Nuclear Science and Technology Organisation (ANSTO).

For stable isotope analysis 0.15mg of each powdered sample was loaded into tin capsules and compacted manually to remove air spaces. The isotopic analysis was conducted at ANSTO in Sydney, Australia, using a continuous-flow isotope ratio mass spectrometer (CF-IRMS) model Delta V Plus (Thermo Scientific Corporation, U.S.A.), interfaced with an elemental analyser (Thermo Fisher Flash 2000 HT EA, Thermo Electron Corporation, U.S.A.). All data were reported relative to IAEA (International Atomic Energy Agency) secondary standards, and were certified relative to air for nitrogen, and Vienna-PeeDee Belemnite (VPDB) for carbon. A two-point calibration was used to normalise the data, using standards (Chitin and Caesin Sodium Salt from Bovine Milk), which bracket the analysed samples. Both of these standards were used as quality control references and were included in every sample run. All results were accurate to 1% for both C% and N%, and ±0.3 parts per thousand (‰) for δ^{13}C and δ^{15}N; they were reported in delta (δ) units in parts per thousand (‰) determined by the formula:

$$X(‰) = \left(\frac{Rsample}{Rstandard} - 1\right) \times 1000$$

4.2.2 Soil organic carbon and radiometric dating

Soil coring for soil organic carbon and radiometric dating was undertaken with a Russian D-Core to allow for easy trapping of wet material, capturing depths of 0-100cm. Five cores were taken at each of the two sites, one in each of the five aboveground biomass plots. All cores were placed in cool storage and transported to the laboratory. Cores were then sectioned and dried in the oven at 60°C for 72 hours. Bulk soil samples were then homogenised with a mortar and pestle. Samples were prepared for ^{210}Pb and stable isotope analysis at ANSTO facilities, and Loss-on-Ignition (LOI) at

Macquarie University. [210]Pb samples were sectioned at 0.5cm intervals for precision, to a depth of 20.5cm. Stable isotope samples were sectioned at 1cm intervals to a depth of 10cm, 2cm intervals to a depth of 30cm, and 5cm intervals to a depth of 100cm, and every second sample was analysed. Following Schlacher and Connolly, (2014), the champagne test was used for each sample to reveal whether material contained inorganic carbon. All tests returned an absence of carbonates, thus %C is equal to %OrgC and hitherto referred to as %C. The same depth intervals were used for secitoning LOI samples, however every sample was analysed. See Figure 15 for detailed sectioning and preparation of cores for analysis.
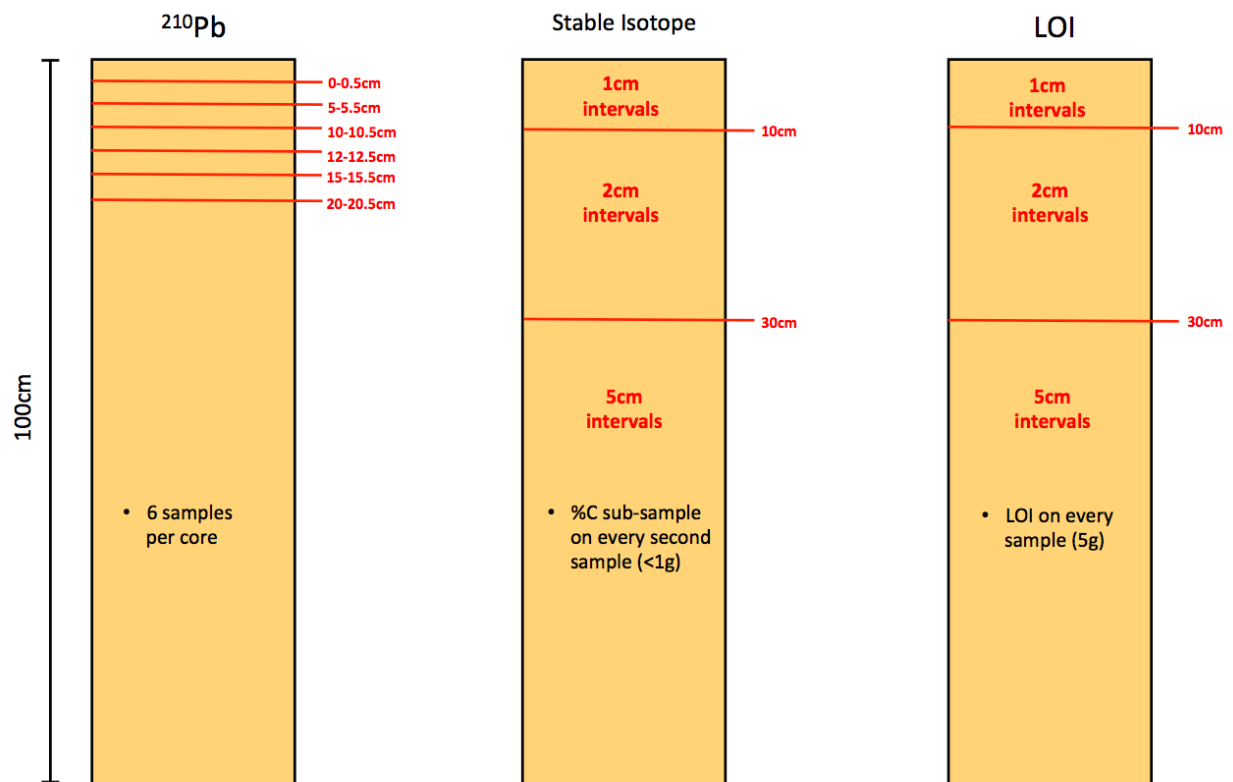
Figure 15: Visual representation of sectioning and preparation of cores for analysis.

[210]Pb was specifically selected to (i) allow for an estimation of carbon accumulation using a standard method and (ii) identify the depth at which Saintilan was sampling in 1989, to identify belowground compartments above and below this horizon. Carbon from samples were converted to CO_2 using the sealed-tube method Hua et al., (2001)

with CO_2 then converted to graphite by reduction using excess hydrogen in the presence of an iron catalyst at 600°C for 12 hours. Once completed, the graphite and iron mixture was pressed into aluminium cathodes for ^{14}C measurement by Accelerator Mass Spectrometry at ANSTO, following methods outlined in Fink et al., (2004). Dates are reported as conventional radiocarbon ages. %C was assessed using both LOI and elemental analysis applied to ^{210}Pb results to generate carbon accumulation rates.

5. Results

5.1 The 1989 horizon marker

The age and depth of sample material was plotted showing gradual accretion at both sites, with a slight accelerating trend at S2. The ^{210}Pb data was considered a reliable guide in determining the depths at which Saintilan (1989;1995) would have been sampling, calculated to be 12cm below the contemporary surface in S1, and 13cm below the contemporary surface in S2. These depths are assumed to be those from which Saintilan (1989;1995) took the original measures, and were used as a point of comparison between the past data set and the current data set (conceptualised in Figure 14, p. 21) - referred hitherto as the 1989 horizon.
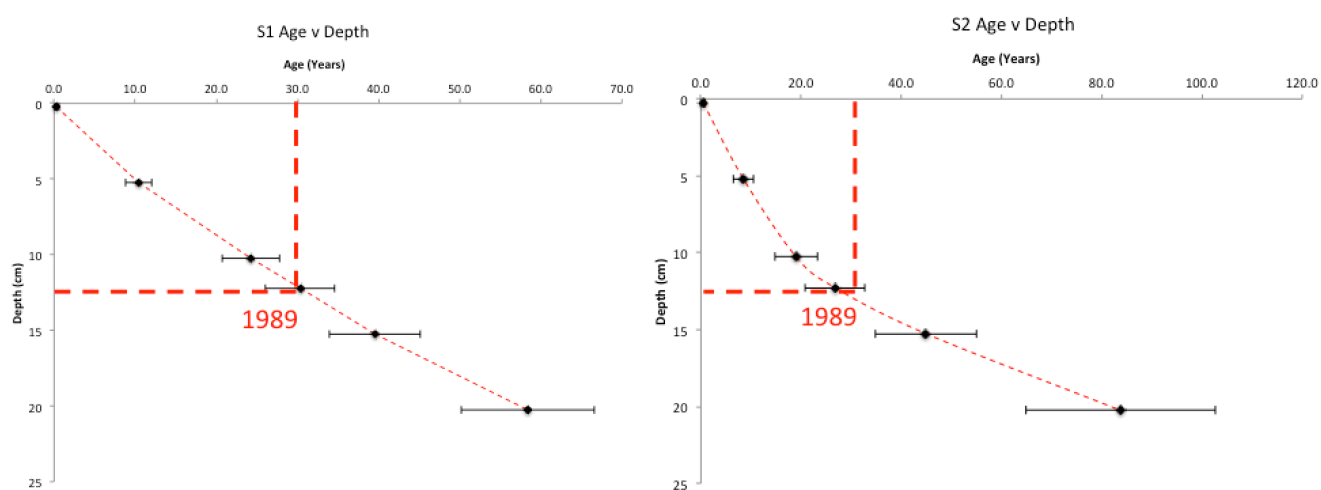
Figure 16: Sedimentary radiometric age plotted against depth in S1 and S2.

5.2 Aboveground biomass

A significant increase of aboveground biomass over the 30-year period can be seen in both S1 and S2 since the original measures were taken.
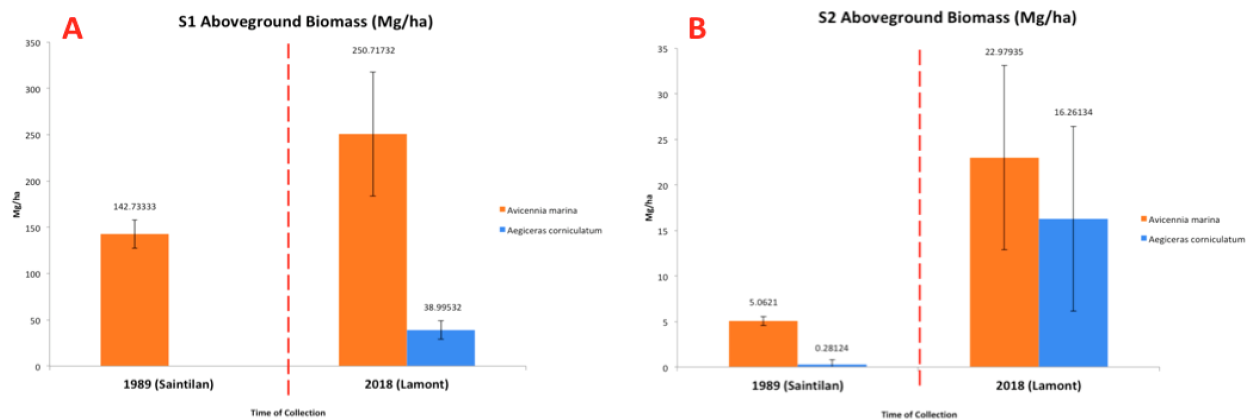
Figure 17: Comparison of aboveground biomass measures in S1 and S2 from 1989 to 2018.

S1, the tall mangrove forest, shows a higher biomass than S2. This can be attributable to (i) significant increase in size of the trees in S1 and (ii) increased density of trees in S1. Current plot data compared to the past plot data in S1 indicates that not only has the biomass increased in height and DBH, but the number of trees has also increased. This increased size and density contributes to a higher biomass in S1. S2 biomass has also changed since 1989, where DBH has increased, yet height remains relatively similar. However, *Ae. corniculatum* data in S2 is not directly comparable, as the 1989 survey only recorded one tree (original 16m^2 plot), thus there is limited spatial variability.

Table 6: Comparison of aboveground vegetation survey results 1989-2018. Units of meaurements: density = number of trees per 100m^2 in 1989 (standardised from original 16m^2), and per 25m^2 in 2018 (standardised from original 16m^2), height = metres (average), DBH = centimetres (average).

	Density *A. marina*	Density *Ae. corniculatum*	Height *A. marina*	Height *Ae. Corniculatum*	DBH *A. marina*	DBH *Ae. corniculatum*
S1 1989	18.8 ± 10.8	-	8.5 ± 0.3	-	58.6 ± 3.1	-
S1 2018	9.8 ± 4.4	2.6 ± 2.0	10.4 ± 0.4	3.9 ± 0.4	61.9 ± 4.4	8.6 ± 0.8
S2 1989	54 ± 31.9	2.1 ± 3.6	2.1 ± 0.1	1.5 (n=1)	8.8 ± 0.5	1.3 (n=1)
S2 2018	44.8 ± 40.6	76 ± 12.3	1.9 ± 0.1	1.2 ± 0.04	9.6 ± 0.9	10.6 ± 1.0

S1 remains a relatively homogenous forest, predominantly populated with *A. marina*. In comparison, S2, which was initially a mudflat populated with salt marsh, has now become a mixed species forest, where a significant increase in the density of vegetation can be seen (almost a doubling of *A. marina* density, and an invasion of dense *Ae. corniculatum*). The number of trees in S2 far outweighs the number of trees in S1, which may suggest that as S2 reaches full maturation, aboveground biomass will be adjusted by a combination of tree growth and self-thinning.

5.3 Belowground root biomass

Similar to the aboveground biomass changes, an increase in belowground root biomass can be seen since the original measures were taken. Thirty years ago, S1 had a larger biomass compared to S2, most likely due to S1 being populated with mature, tall trees and S2 being a newly recruited forest of juveniles. However, since 1989, S2 has increased significantly in root biomass and has now surpassed S1. This may be attributable to the rapidly recruiting and dense population of young, *A. corniculatum* in S2, and the doubling of *A. marina* density at the site over 30 years. Compared to aboveground biomass, as seen above, there is a significantly larger amount of belowground

Figure 18: Comparison of belowground root biomass measures in S1 and S2 from 1989 to 2018.

biomass in both sites, suggesting that there is a vast network of root material beneath the surface. Figure 18 shows that not only has there been an increase of new root material above the 1989 horizon, but there has also been an expansion and

development of new deep root material below the 1989 horizon. This indicates that not only has new root material been introduced on top of the surface from which Saintilan took the original measures, but that deep root material below the 1989 horizon has continued to expand and increase in mass, and that this dominates comparisons of root mass between the two time periods.

5.4 Belowground %C

Figure 19: Belowground %C in S1 and S2, measured in 2018.

Using elemental analysis, %C was calculated in two cores, one at each site. A gradual, increasing trend can be seen in both S1 and S2, where total %C increases towards the surface. This is reflected in Figure 19, where the shallower depths (closer to 2018) show higher concentrations of carbon, compared to the deeper depths (closer to 1989) where concentrations are lower. This indicates that as time passes, carbon continues to be buried belowground, creating a larger stock over time. However, it is important to note that a large proportion of the carbon seen in the shallower depths is most likely fresh carbon that has been deposited recently, either through near-surface root growth (i.e. autochthonous) or tidal deposition of allochthonous carbon. It is unknown how much of this freshly accumulated carbon will actually remain and be preserved as blue carbon as time passes, and how much will be lost to external factors within the carbon cycle. Thus, it is not certain if permanent, stored carbon is increasing with time and not just temporary surface carbon, and whether or not %C will continue to increase through time, despite this increasing trend seen in Figure 19.

5.5 Belowground %OM

Similar to %C, a gradual, increasing trend can be seen in belowground percent organic matter (%OM), where the shallower depths show higher levels of %OM and the deeper depths show lower levels of %OM. Despite the occasional anomalies, it can be seen that over the 30-year decadal timeframe, %OM has steadily increased in both sites, which has contributed to increased %C levels as seen in Figure 19. Belowground root biomass increase (Figure 18), has likely had an influence on this steady increase. Again, it is important to note that is it unknown how much of this organic matter will remain within the system, and how much will decompose and eventually release the trapped carbon. Thus, despite this gradual increase, it is difficult to predict whether or not %OM will continue to increase through time, furthering complications in determining whether carbon stocks will increase over a temporal scale.

Figure 20: Belowground %OM in S1 and S2, measured in 2018. C2 – C5 is Core 2 to Core 5.

5.6 Comparison of coring and trenching methods

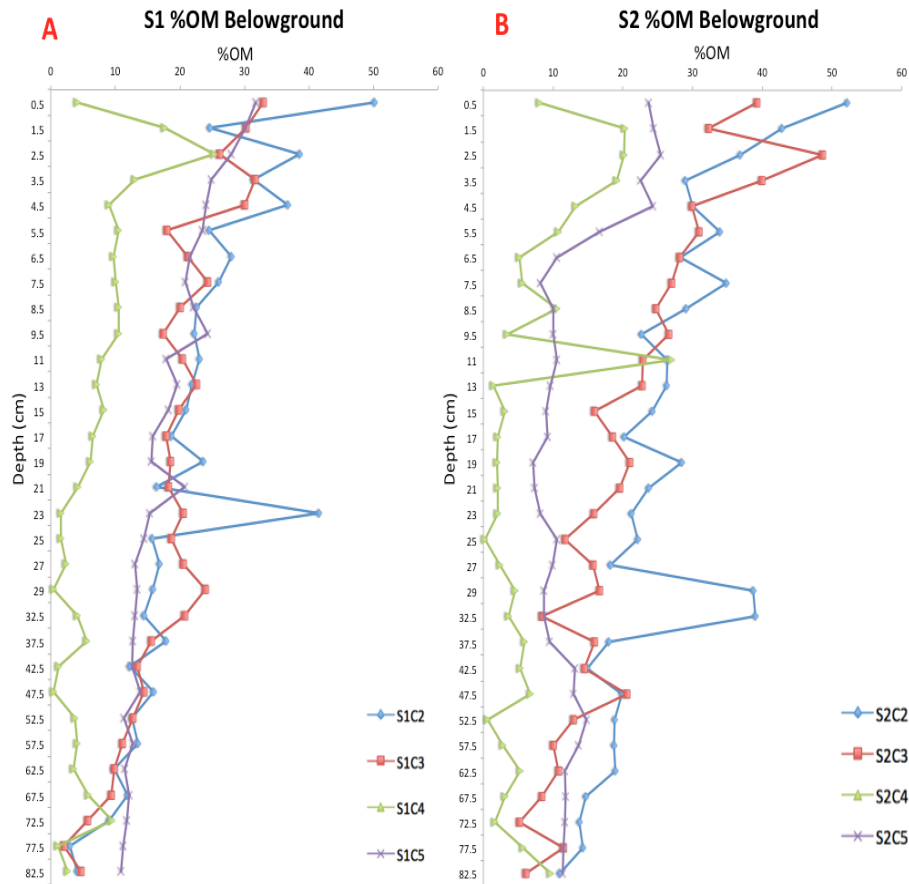The carbon stock of root biomass (collected through trenching) was calculated using %C results from elemental analysis on ten sub-samples. The carbon stock in bulk biomass (collected through coring) was calculated through a linear regression of the relationship between %C results and %OM results (Figure 21).
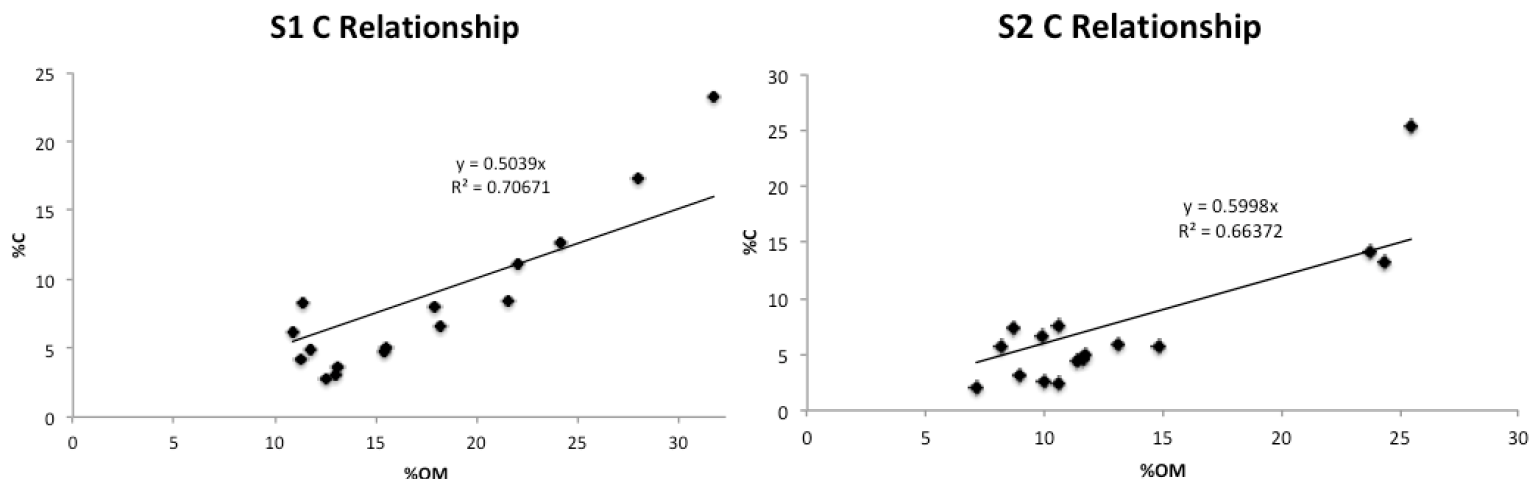
Figure 21: Relationship between %C and %OM. Both sites show a strong relationship between the two variables, with an R^2 value of above 0.6. Due to the complex nature of mangrove ecosystems (intricate root systems belowground), a value of 0.59 is considered strong (Blue Carbon Manual, Howard et al. 2014).

As expected, the coring method returned higher values of belowground carbon, as it captured both soil and root carbon, whereas the trenching method was only used to capture whole root carbon, see Figure 22 below. Despite this, the trench method may be a more reliable sampling method as it can also be used to capture bulk material, and would capture a larger volume of material. For this study, bulk material collected through trenching was drained through a sieve, and only the remaining root material was collected. This was done to replicate the past measures completed by Saintilan, (1995). However, considering Figure 22, even when the bulk material was drained, the trench method shows a carbon stock that equates to almost half of the carbon stock measured from the coring method. The ratio of root carbon to bulk carbon in S1 is 0.615 above the 1989 horizon, and 0.434 below the1989 horizon. The ratio of root carbon to bulk carbon in S2 is 0.57 above the 1989 horizon, and 0.435 below the 1989 horizon – a

remarkable consistency between sites. This indicates that approximately half of the belowground carbon is stored in living root material, or recently dead roots that are being sampled as living material. This reiterates the significance of root material in mangrove ecosystems and its role in belowground carbon capture. Studies that do not quantify root material but are estimating blue carbon stocks, are likely underestimating the total amount of stored carbon.
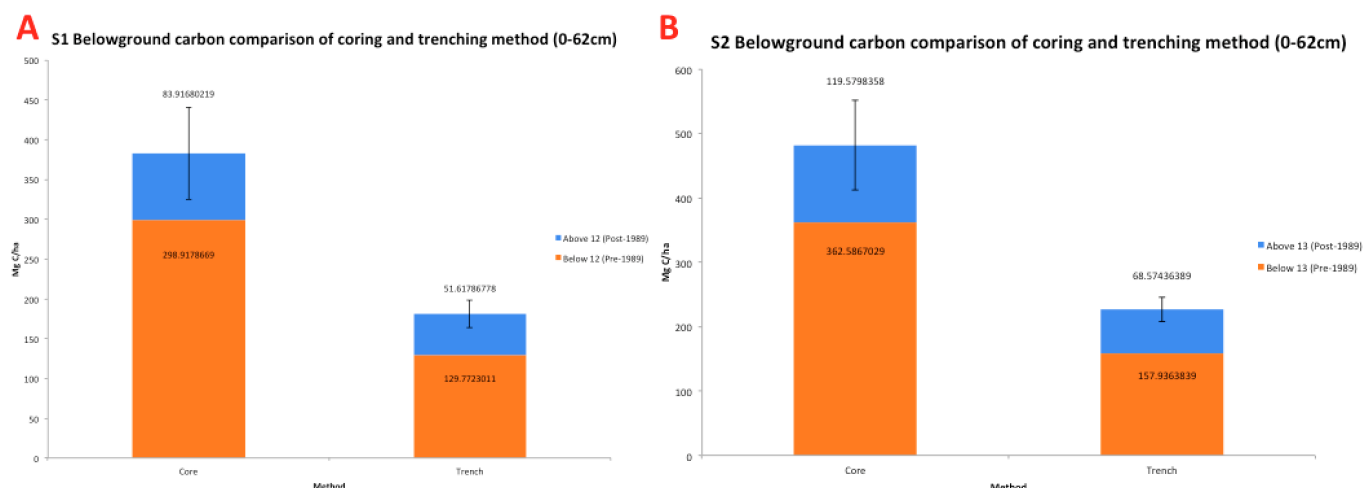
Figure 22: Belowground carbon comparison of coring and trenching method in Mg C ha^{-1}, taken in 2018.

5.7 Carbon accumulation rates
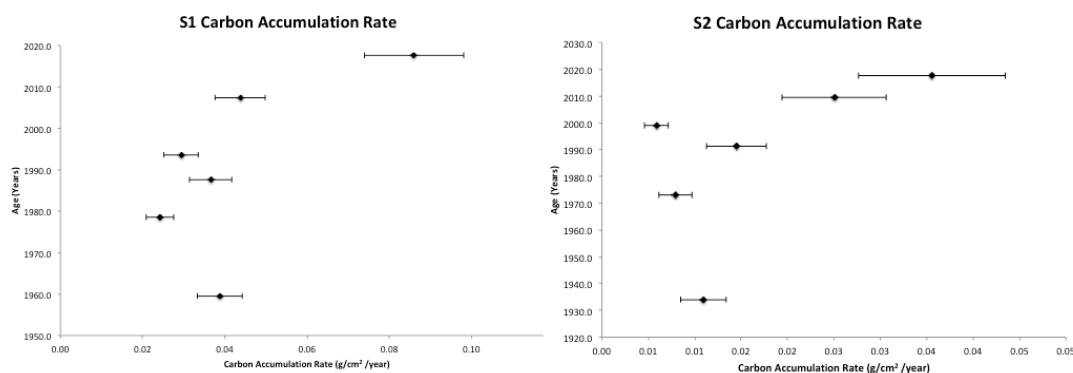
Figure 23: Carbon accumulation rates in S1 and S2, taken in 2018.

Both S1 and S2 show a similar trend in carbon accumulation rates over recent decades, as judged by radiometric dating, though the S1 rate is substantially higher. Following the year 2000, carbon accumulation rates in both S1 and S2 continue to steadily increase to

the present. However, there are two assumptions implicit in the interpretation of carbon accumulation rates using radiometric dating, both of which might be challenged. First, the higher density of carbon at surface does not necessarily mean that contemporary root accumulation is greater, because it does not factor in the decay of old root material in the profile. Earlier periods may well have had equally strong surface root accumulation but suffered poor preservation. It is highly likely that high %C (and consequently, high carbon accumulation rates) in near surface layers are a function of the high concentration of fresh fine root material, much of which will decay over time as these layers become deeper in the profile.

Second, it is important to remember that these methods do not reveal the age of the carbon, but rather the age of the sediment, and contemporary root material might be incorporated at any depth within the profile. Our repeat measures show a very strong increase in root density below the 1989 horizon at both sites, to the extent that contemporary root material may be a dominant source of carbon across the entire profile. This makes estimation of carbon accumulation rates using radiometric dating a serious under-estimation of the actual rate (discussed more fully in section 5.9 below).

5.8 δ^{13}C signatures of root biomass

All bulk sediment samples showed a consistent δ^{13}C soil organic carbon signature between -25.8% to -27.9%, (mean -26.9% at S1; -26.4% at S2: Table 7). This consistency indicates that root material (δ^{13}C range -26.3% to -27.9%) plays a strong role in carbon accumulation and that autochthonous carbon is likely the dominant source of blue carbon preserved within the mangrove ecosystems at this site. Leaves of both species are depleted compared to the roots, suggesting a lesser contribution of leaf material to belowground carbon stocks, and underscoring the importance of distinguishing between leaf and root carbon in the development of proxies (Kelleway et al., 2018).

Table 7: Averages of δ^{13}C signatures in bulk material, root material, and leaf material, all showing consistency within similar ranges.

Site	δ^{13}C Bulk	δ^{13}C Root	δ^{13}C Leaf
Site 1 Tall	-26.9%	-27.0%	-27.3% (*A. marina*)
Site 2 Stunted	-26.4%	-26.7%	-28.6% (*A. corniculatum*)

5.9 Overall temporal changes

5.9.1 Radiometric analysis

Results show that S1 has a higher carbon stock than S2, and accumulates carbon at a faster rate as estimated by radiometric dating. Despite this, S2 has experienced a faster increase in root mass and maintains a higher root mass than S1, see Table 8. Higher carbon stock and carbon accumulation rates in S1 can be attributed to larger and older aboveground biomass in the forest. Again, it is important to emphasise that these results were derived from radiometric dating, and do not necessarily show an accurate rate of accumulation given evidence of deep root penetration. In particular, the estimated rate of carbon accumulation at S2 would be an underestimate, given the proportion of new (post-1989) material added below this radiometric horizon.

Table 8: Accretion and carbon accumulation in S1 and S2, taken in 2018, derived from radiometric analysis.

	S1 Tall	S2 Stunted
Bulk Sediment Rate (Mg ha^{-1} y^{-1})	37 ± 5.2	25.1 ± 5.6
C Accumulation Rate (Mg C ha^{-1} y^{-1})	4.3 ± 1	1.7 ± 0
Post-1989 Bulk Accretion (Mg ha^{-1})	1073 ± 150.8	727.8 ± 162.4
Post-1989 C Accretion (Mg C ha^{-1})	124.7 ± 29	49.3 ± 0
%C	43%	32%

5.9.2 Repeat measure analysis

Repeat measures provide an insight into change in above and belowground biomass over time, useful in the interpretation of carbon stock changes. Figure 24 (a) and (b) populate the carbon store comparison of Figure 14 (p. 21), with measured values for sites 1 and 2 respectively.

A   **Site 1 Tall**

2018 Sampling

1989 Sampling		

Above-ground biomass 2018 (x') **290 Mg/ha**	30 yr above-ground sequestration (a) = x' - x

Above-ground biomass 1989 (x) **143 Mg/ha**

Root mass below 1989 surface in 1989 (y) **90 Mg/ha**

Root mass above 1989 surface in 2018 (y") **146 Mg/ha**

= **147 Mg/ha**

30 yr root mass accumulation (b)= y"+ y' − y

= **422 Mg/ha**

Root mass below 1989 surface in 2018 (y') **366 Mg/ha**

30 yr autochthonous accumulation = a + b

= **567 Mg/ha**

B   **Site 2 Stunted**

2018 Sampling

1989 Sampling

Above-ground biomass 2018 (x') **40 Mg/ha**

Above-ground biomass 1989 (x) **5 Mg/ha**

Root mass below 1989 surface in 1989 (y) **55 Mg/ha**

Root mass above 1989 surface in 2018 (y") **193 Mg/ha**

30 yr above-ground sequestration (a) = x' - x

= **35 Mg/ha**

30 yr root mass accumulation (b)= y"+ y' − y

= **583 Mg/ha**

Root mass below 1989 surface in 2018 (y') **445 Mg/ha**

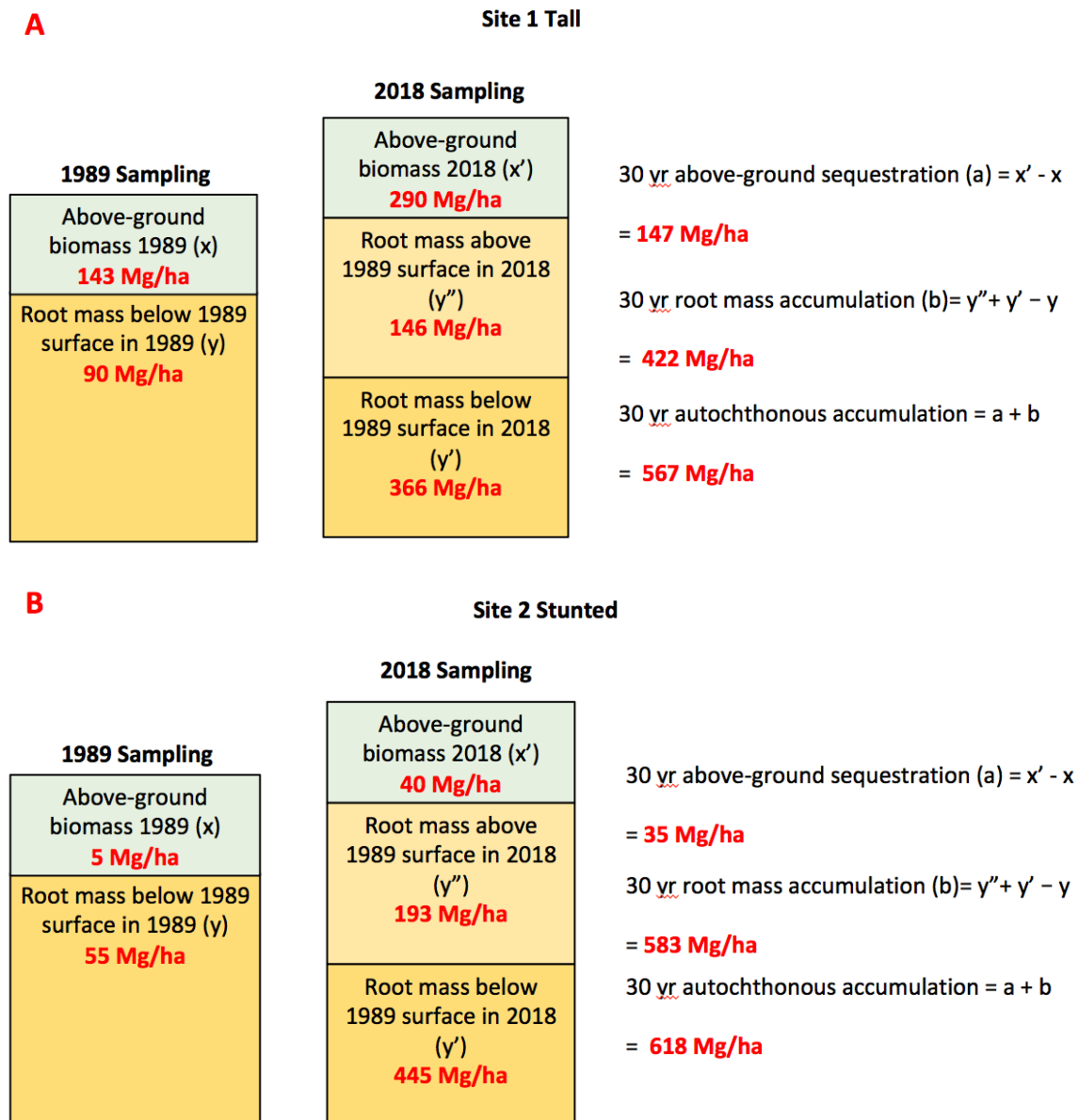30 yr autochthonous accumulation = a + b

= **618 Mg/ha**

Figure 24: S1 (a) and S2 (b) visual representation of biomass stock change.

Above and belowground biomass site-wide has increased since 1989, where aboveground biomass has increased by 147 Mg/ha in S1 and 35 Mg/ha in S2 – a ~2x and ~8x increase respectively. Belowground root mass has increased by 422 Mg/ha in S1 and 583 Mg/ha in S2 – a ~5.5x increase and ~10x increase. Although increases can be seen in both forests, S2 shows a far more rapid increase compared to S1, and also shows larger carbon stocks. Aboveground biomass has more than doubled over the 30-year period in S2, and still being a newly recruited forest, it is likely to continue to increase through time as the forest matures. Furthermore, despite having a lower aboveground biomass, S2 has significantly larger root mass compared to S1, indicating that belowground roots likely play a key role in storing carbon beneath the surface.

The overall *in-situ* accumulation in biomass is 567 Mg/ha in S1 and 618 Mg/ha in S2 since 1989, demonstrating the key role autochthonous material plays in contributing to, and preserving long-term blue carbon. Figure 24 also demonstrates that root mass continues to increase below the 1989 surface. This shows that deep root material stores much larger mass compared to shallower depths, where there has been lesser addition of roots above the 1989 horizon. Unfortunately, Saintilan did not measure bulk carbon stocks when collecting data, thus we do not have an exact comparison of how much bulk carbon has accumulated since 1989. What is also unclear, is how much of this buried carbon will remain within the system, and how much allochthonous input there was to the study area, as neither of these variables were measured for the study.

5.9.3 Comparison of radiometric analysis and repeat measure analysis

Figure 25 shows the best estimates of a carbon budget for the Spencer study site using available data for each site. There is an evident increase in root carbon, post-1989 shallow root carbon, as well as deep root carbon continuing to accumulate below the 1989 horizon marker. Bulk carbon was not measured by Saintilan, thus there is no direct comparison, however it can be seen that bulk material stores significant quantities of belowground carbon based on 2018 measures. What would have enhanced the study's results would be estimates of how much allochthonous input there is to carbon

storage, as well as how much carbon is being lost through external forces. Without estimates of these two variables, there is still uncertainty in what variables are influencing carbon stock again, and how much of the measured carbon will remain stored belowground. We have constrained the estimate of allochthonous input by considering the difference between bulk carbon in 2018 above the 1989 horizon, and our knowledge of the root contribution to this figure.
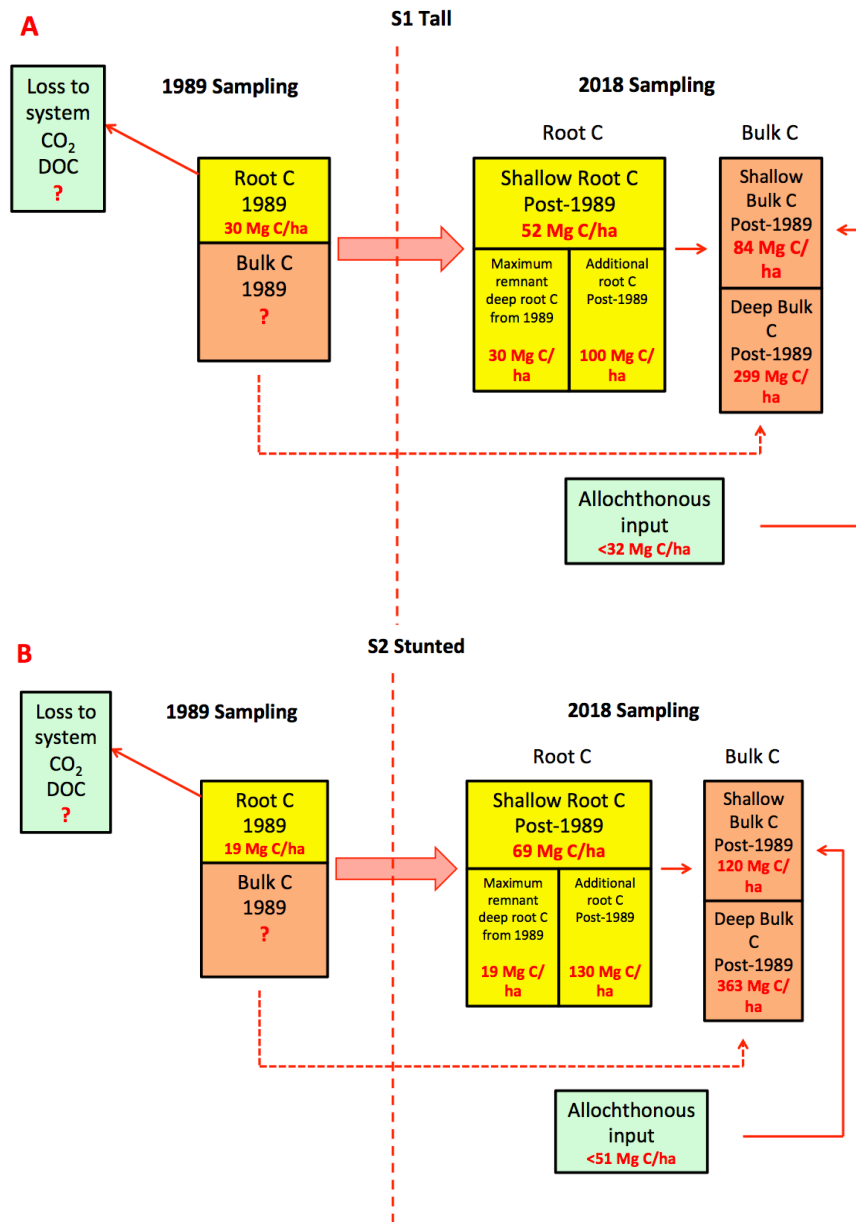

Figure 25: Flow-chart of belowground carbon dynamics over the 30-year studied timeline. Carbon values in 1989 are derived from Saintilan (1989;1995). Root carbon values in 2018 are derived from pit trenching results, and bulk carbon values in 2018 are derived from bulk core elemental analysis.

Our carbon budget for the sites suggest that nearly half of current bulk carbon can be explained by additional root production since 1989. In S1, 152 Mg C ha^{-1} of the 383 Mg C ha^{-1} stored is increased belowground root production, and in S2, 199 Mg C ha^{-1} of the 483 Mg C ha^{-1} stored is increased belowground root production. This demonstrates the significant role belowground root expansion plays in blue carbon storage. Repeat measure root carbon accumulation rates were calculated, through the following:

$$x = \left(\frac{2018 \; root \; carbon - 1989 \; root \; carbon}{30 \; years} \right)$$

Overall, it was found that the root carbon accumulation of 5.06 Mg C ha^{-1} y^{-1} in S1 and 6.63 Mg C ha^{-1} y^{-1} in S2, determined by repeat measure analysis, is greater than the estimate of *bulk carbon* determined by radiometric analysis - only 4.3 ± 1 Mg C ha^{-1} y^{-1} in S1 and 1.7 ± 0 Mg C ha^{-1} y^{-1} in S2, see Table 9. Unfortunately Saintilan (1989;1995) did not measure bulk carbon, so we are unable to estimate the repeat analysis bulk carbon accumulation rates. Considering the repeat analysis of only root carbon exceeded radiometric analysis of bulk carbon, it is likely that significantly higher estimates of carbon accumulation could be generated through repeat analysis of bulk carbon material. It is interesting to note that radiometric analysis estimates found that S1 carbon accumulation rates were higher than S2, by a significant margin, whereas repeat measure analysis found that S2 had higher root carbon accumulation. Radiometric analysis is therefore significantly underestimating carbon storage estimates in the literature, and should be reconsidered as a sole method of carbon quantification.

Table 9: Comparison of carbon accumulation rates derived through radiometric analysis and repeat measure analysis. A larger estimate was calculated through repeat measure analysis, indicating radiometric dating is underestimating carbon storage in the literature.

	S1 Tall	S2 Stunted
Radiometric analysis Bulk Carbon (Mg C ha^{-1} y^{-1})	4.3 ± 1	1.7 ± 0
Repeat analysis Root Carbon (Mg C ha^{-1} y^{-1})	5.06	6.63

6. Discussion

6.1 Methodological comparison

The study has shown that the reliance on radiometric methods can underestimate carbon accumulation estimates, and verifies that repeat measures through time provide important insights into quantifying temporal carbon stock change. Radiometric dating assumes that carbon does not accumulate below sediment once it has been deposited, creating inconsistencies and underestimations in carbon stocks. Our results show that carbon accumulation rates were underestimated by at least 0.76 Mg C ha^{-1} y^{-1} in S1 and 4.93 Mg C ha^{-1} y^{-1} in S2 using this method. This means radiometric dating has conservatively resulted in a 15% and 74% underestimation in overall carbon accumulation rates at S1 and S2 respectively, raising broader implications about the reliability of radiometric analysis in the literature. Our estimates from radiometric analysis are fairly consistent with estimates in the literature. Osland et al., (2012) estimated a rate of 2.18 Mg C ha^{-1} y^{-1} in a mangrove-encroached salt marsh in Florida, USA, Lunstrum and Chen, (2014) estimated 1.55 Mg C ha^{-1} y^{-1} in a mangrove forest in China, Asia, and Marchand, (2017) estimated 2.3 Mg C ha^{-1} y^{-1} in a mangrove forest in French Guiana. S1 rates were higher than these reported in the literature, whilst S2 rates were lower. Looking more closely at South-east Australia, Saintilan et al., (2013) created a dataset of 7 separate study sites in the region, ranging from Southern Victoria to Northern New South Wales, and estimated an average of 2.50 Mg C ha^{-1} y^{-1}. Again, this estimate in the literature falls within our ranges of radiometric results, where the S1 rate was higher, and the S2 rate was lower. However, these estimates are significant underestimations when compared to our repeat measure analysis results. The highest estimation, from Saintilan et al., (2013) is only 2.50 Mg C ha^{-1} y^{-1}, below the 2.56 Mg C ha^{-1} y^{-1} estimated for S1 and 4.13 Mg C ha^{-1} y^{-1} for S2. Again, these estimates are only of root carbon, indicating that the bulk rate would be even higher. This strongly suggests that carbon accumulation rates in the literature are being significantly underestimated, particularly in locations of vegetation change.

Most importantly, this method underestimates the key contributor to blue carbon stores - root biomass material, as it cannot analyse biomass that continues to expand below the surface of sediment deposition. Radiometric dating is a useful tool in finding points in time and estimating rates of carbon accumulation, but this study shows that it is not the most effective approach to quantify carbon through time. Although space is often used as a substitute for time, and radiometric dating can fill in missing blanks, replicating measures has been shown to build a robust estimate of carbon storage over time, although both root carbon and bulk carbon should be measured. Together they provide the most reliable information on how carbon store has changed and may change into the future. Radiometric dating can be used, as in this study, to compared surface carbon accumulation with new root carbon introduced at depth, providing additional resolution to repeat measure datasets.

6.2 Significance of root biomass

Comparative repeat measures show that carbon stocks have increased over the 30-year period, with the largest increase found in belowground biomass. Most importantly, the increase in belowground biomass is making an important contribution to belowground carbon store, as indicated by two lines of evidence. First, soil organic carbon $\delta^{13}C$ is consistently in the range of contemporary mangrove root material. Second, the measured accumulation in belowground root mass, converted to Mg C ha^{-1}, contributed to more than half of the measured contemporary belowground carbon. Given questions being rased about carbon provenance (Kelleway et al., 2018; Maher et al., 2017), this demonstration of the dominant contribution of autochthonous mangrove root production is encouraging, and suggests a method that could usefully be applied to measuring additionality associated with afforestation and other blue carbon programs. It remains to be understood what controls are driving this huge increase in belowground root material, and how it is likely to change with time.

6.2.1 Relationship with aboveground biomass

Mangrove forests are complex ecosystems with highly intricate root structures belowground. It is argued in the literature, although in a more limited sense compared to bulk material, that these dense belowground root systems allow mangroves to capture and preserve much larger stores of carbon belowground - often exceeding aboveground carbon storage (Comley and McGuinness, 2005; Komiyama et al., 2008; Njana et al., 2015). A major control on the expansion and maintenance of this network is the aboveground biomass. Tree density has been explored as a contributing factor to accumulating belowground root material. Adame et al., (2017) compiled 7 studies in the literature and found that the highest root biomass is in densely populated forests, with trees that have small DBH measures. This may explain why S2 has a higher mass of belowground root material, as S2 is a very densely populated forest, with an average DBH of 10.3cm. Compared to this, S1 is a mature, yet sparse forest, with significantly larger trees with an average DBH of 54.6cm (Table 6). Similar findings of correlation between high tree density aboveground and high root density belowground in other areas of the world have been reported (Komiyama et al., 1987; Lang'at et al., 2013; Tamooh et al., 2008), emphasising the influence of aboveground biomass on root material. Species mix and richness of aboveground biomass has also been argued to increase root mass. Lang'at et al., (2013) found that forests with mixed species developed denser root networks belowground at faster rates compared to homogenous forests, and within 3 to 4 years, belowground biomass had exceeded aboveground biomass. This is a comparable scenario to our own findings, as S2 is a mixed species forest which has accumulated root biomass at a significantly fast pace for a stunted forest, and belowground biomass has exceeded aboveground biomass in both sites. Lang'at et al., (2013) also found that the presence of *A. marina* was a strong contributor to root biomass development, as it is a fast-growing species that helps expand the belowground network at a quicker pace over time compared to other species. Pairing *A. marina* with other species was therefore found to have complimented overall biomass growth. This could also explain why S2 experienced such rapid growth over such a short period of time, as the stunted forest experienced significant change when *A.*

41

cornciulatum began to encroach on the relatively bare, homogenous mudflat. It is also important to note that many of the individuals in S2 recruited recently, as evidenced by comparison with the density and floristics of the Saintilan (1989;1995) survey. This strong recruitment may be influencing rapid biomass development, as there is evidence to support that maturing trees develop root biomass at faster rates than mature trees (Tamooh et al., 2008). This may also explain why S2 is gaining such high levels of carbon despite being a stunted forest.

Mangrove encroachment is therefore an important reason why S2 experienced such rapid rates of carbon accumulation. Doughty et al., (2016) found that mangrove encroachment of saltmarsh in Florida led to increases in carbon stock, although primarily in aboveground biomass rather than belowground biomass. They found that encroachment of mangrove onto saltmarsh increased carbon stocks by 22% over 7 years in ecotonal wetlands. S2 is an active encroachment zone, with mangroves initially colonising between 1945 and the first biomass survey by Saintilan in 1989, but substantial encroachment and thickening has occurred since then, see Figures 10, 11 and 12 above. Our results suggest that this has led to substantial increases in soil carbon above and belowground, driven by strong increases in root and shoot biomass. This finding is of regional significance, given that Saintilan and Williams, (1999) found that significant losses of saltmarsh were evident in Queensland, New South Wales, Victoria and South Australia over a 50-year period, and mangrove forests were invading landward and replacing these ecosystems. The results reported here suggest that the encroaching mangrove replaced the relatively bare mudflat, with a dense, mixed-species forest, capable of storing large quantities of carbon. Saintilan et al., (2014) estimated that 30% of saltmarsh was lost to mangrove encroachment in Southeast Australia, emphasising the rapidly expanding dominance of mangrove forests within the area. More recently, Kelleway et al., (2016a) found that 70 years of mangrove encroachment onto saltmarsh habitats had increased carbon stocks in tidal wetland ecosystems, but that statistically significant changes in belowground carbon store could not be detected until after 30 years of colonisation by mangrove. It was estimated that belowground carbon stocks increased at 2.3 Mg C ha^{-1} y^{-1} as mangroves invaded salt

marsh habitats, which was extrapolated to a total belowground carbon stock of 7155 Mg C y^{-1}, and overall increase of 500 864 Mg C over 70 years. Our estimated belowground carbon stock was 8.6 Mg C ha^{-1} y^{-1}, about 3.7 times higher. Following Kelleway et al., (2016a) this was extrapolated to the entire region of mangrove encroached forests in New South Wales. We refine this estimate and suggest that encroachment has contributed increases of ~1,853,000 Mg C over the 70 years for which mangrove encroachment has been observed in the state, not including the substantial increase in aboveground carbon stocks.

Our results comparing root mass between 1989 and 2018 confirm that accumulation of belowground root mass may increase substantially for several decades after initial colonisation. The vegetation dynamics of S2 is therefore likely to have enhanced the forest's carbon capture potential, and may explain why it has lead to substantial carbon sequestration in spite of (i) limited tidal inundation (Figure 13) and (ii) the potential for soil oxidation and carbon remineralisation. Belowground biomass results also indicate that S2 has significantly higher levels of root biomass compared to S1, further suggesting that S2 is capable of storing larger stocks of carbon, at faster rates through time. Blue carbon afforestation projects could therefore consider development of dense, mixed-species forests to help facilitate root mass expansion belowground. These aboveground vegetative characteristics have been found to be a key control on root mass accumulation over the 30-year study period, and plays a crucial role in maintaining long-term blue carbon preservation in mangrove ecosystems.

6.2.2 Nutrients, resource availability, and mangrove root biomass

The availability of nutrients and resources for trees within a mangrove forest, as well as environmental stressors such as hydroperiods, salinity levels and atmospheric CO_2, can all influence the root biomass network belowground, which in turn, affects carbon storage. Nutrient availability has been linked with belowground root biomass growth, where phosphorus (P) deprived forests in Micronesia and the US have been shown to have denser fine root mass (Castañeda-Moya et al., 2011; Cormier et al., 2015).

However, contrary to this, P enriched forests in Mexico have also been shown to have high root mass (Adame et al., 2014), and Hayes et al., (2017) found that both nitrogen (N) and P enrichment has resulted in increased root growth in Queensland, Australia. Despite the opposing findings, it can generally be agreed that the nutrient limitation, influences mangrove forests to increase their root to shoot ratio and enhance root production to capture and retain nutrients more efficiently - a means to adapt to the environmentally harsh conditions (Adame et al., 2017; Naidoo, 2009). It is uncertain how nutrients impact root growth in this study, as it was not measured. Water level logger data, Figure 13 above, shows that S2 has limited tidal flows compared to S1, suggesting that the S2 forest may be nutrient deprived as lesser amounts of sediment are being transported allochthonously, and a higher potential for gaseous dentrification. This may be influencing higher rates of root expansion, and therefore belowground carbon, however further study in nutrient levels would need to be completed to verify this.

Figure 13 also shows that S2 experiences minimal tidal inundation frequency, due to its geomorphic setting on an intertidal mudflat at higher elevation. Adame et al., (2017) found in the literature that low inundation frequency and high salinity levels result in stunted aboveground growth, but enhanced belowground root mass growth. Saintilan, (1997), found similar results in Spencer, where high salinity levels resulted in stunted aboveground growth, but increased root to shoot ratios. A more recent study, Reef et al., (2015) furthers this by finding that the length of roots in their study were stunted by high salinity levels, but the overall density of the root biomass increased, which allows for higher carbon storage. This is furthered by Liu et al., (2017), who argue high salinity levels and low nutrient availability create an environmentally stressful conditions, which mangrove forests adapt to by increasing root production. This allows the forests to transport water more efficiently, and capture and retain limited nutrients that are available. This may explain the vegetative structure of S2, where the limited tidal inundation frequency yet high salinity levels, have resulted in a stunted aboveground forest, but dense and expansive belowground ecosystem, creating significant stores of preserved blue carbon. Atmospheric fertilisation is also a potential driver of root growth,

where a few studies have detailed how increased CO_2 levels may be preferentially enriching root biomass growth (Reef et al., 2016, 2015; Saintilan and Rogers, 2015).

6.3 Future predictions of temporal change in Spencer study site

Based on the results and findings, we hypothesise the following:

- Aboveground biomass will mature and become denser in S2, resulting in sequestration of larger carbon stocks
- Species diversity will continue to allow S2 to accumulate carbon at significantly faster rates than S1
- Low tidal inundation frequency and high salinity levels will continue to create environmentally favourable conditions for increased carbon accumulation in S2
- S1 will continue to increase in carbon stock and carbon accumulation rates, however at a steadier pace, whereas S2 will experience rapid rates of carbon stock increase and accumulation
- There is an overall assumption that with rising CO_2 levels, atmospheric fertilisation will facilitate an increase in aboveground density, and as a result root carbon - it is unlikely this will tip the balance between the two forests, as it will impact both sites
- The dense belowground root growth may impact surface elevation levels over time, which will have lingering implications on sea-level rise
- Root mass accumulation is likely making an important contribution to soil volume and surface elevation again, which may be resulting in a negative feedback between sea-level rise and carbon sequestration

In order to confirm these speculations, another repeat measure study would need to be completed in the next decade. Another approach would be to replicate this methodology in other locations. This would significantly enhance the scope of the overall temporal monitoring project in the Spencer site, as we would have a data set spanning from 1989 to potentially 2030, 2040 and 2050 - a 60-year repeat measure study, which would

reveal unprecedented insights into long-term carbon storage. The potential of the Spencer study site to be implemented into carbon market schemes is also dependent on environmental management bodies. Blue carbon sequestration cannot be used as a market tool for greenhouse gas abatement, unless we are aware of the long-term carbon dynamics within these sinks (Pendleton et al., 2012). Our findings demonstrate what variables are maximising carbon retention in mangrove ecosystems, and can be applied to management approaches as a means to influence enhanced carbon preservation over time.

7. Conclusions

Overall, the study has found that:

1. Belowground biomass, specifically mangrove root material, plays an integral role in building carbon stocks in a temperate mangrove. Above and belowground biomass increased substantially in a tall gallery mangrove forest and in an upper intertidal mangrove encroachment zone, with most accumulation occurring several decades after initial establishment. This additional post-1989 carbon formed a substantial part of the total carbon pool.

3. Vegetative characteristics, environmental controls and ecosystem age are key influences on long-term temporal carbon storage increase, and needs to be incorporated into management strategy to protect and enhance large blue carbon stocks. Mangrove encroachment led to substantial belowground root mass gains in spite of less frequent inundation, higher salinity and likely lower nutrient levels.

3. Carbon accumulation at both sites was seriously underestimated using radiometric dating alone. This is because most post-1989 additional root material was sequestered below the 1989 sedimentary horizon.

4. Repeat measures at this site successfully demonstrated a substantial gain in autochthonous carbon, and the method, in combination with radiometric dating, could be usefully applied as a robust measure of carbon additionality in blue carbon reafforestation projects.

5. We have revised the estimate of carbon sequestration resulting from mangrove encroachment, upwards to ~1,853,000 Mg C over 70 years of documented encroachment in New South Wales. This figure does not include increases in aboveground carbon stocks.

8. Acknowledgements

9. References

Adame, M.F., Cherian, S., Reef, R., Stewart-Koster, B., 2017. Mangrove root biomass and the uncertainty of belowground carbon estimations. For. Ecol. Manage. 403, 52-60.

Adame, M.F., Teutli, C., Santini, N.S., Caamal, J.P., Zaldívar-jiménez, A., Hernández, R., Herrera-silveira, J.A., 2014. Root Biomass and Production of Mangroves Surrounding a Karstic Oligotrophic Coastal Lagoon. Wetlands 34, 479–488.

Alongi, D., Murdiyarso, D., Fourqurean, J., Kauffman, J., Hutahaean, A., Crooks, S., Lovelock, C., Howard, J., Herr, D., Fortes, M., Pidgeon, E., Wagey, T., 2016. Indonesia's blue carbon: a globally significant and vulnerable sink for seagrass and mangrove carbon. Wetl. Ecol. Manag. 24, 3–13.

Alongi, D.M., 2012. Carbon sequestration in mangrove forests. Carbon Manag. 3, 313–322.

Alongi, D.M., 2014. Carbon Cycling and Storage in Mangrove Forests. Annu. Rev. Mar. Sci 6, 195–219.

Atwood, T.B., Connolly, R.M., Almahasheer, H., Carnell, P.E., Duarte, C.M., Lewis, C.J.E., Irigoien, X., Kelleway, J.J., Lavery, P.S., Macreadie, P.I., Serrano, O., Sanders, C.J., Santos, I., Steven, A.D.L., 2017. Global patterns in mangrove soil carbon stocks and losses. Nat. Clim. Chang. 7, 523–528.

Boon, P.I., 2017. The Hawkesbury River: A Social and Natural History. CSIRO Publishing, Victoria, Australia.

Bouillon, S., Borges, A. V., Castañeda-Moya, E., Diele, K., Dittmar, T., Duke, N.C., Kristensen, E., Lee, S.Y., Marchand, C., Middelburg, J.J., Rivera-Monroy, V.H., Smith, T.J., Twilley, R.R., 2008. Mangrove production and carbon sinks: A revision of global budget estimates. Global Biogeochem. Cycles 22, 1–12.

Breithaupt, J.L., Smoak, J.M., Smith Iii, T.J., Sanders, C.J., Hoare, A., 2012. Organic carbon burial rates in mangrove sediments: Strengthening the global budget. Global Biogeochem. Cycles 26, 1–11.

Castañeda-Moya, E., Twilley, R.R., Rivera-Monroy, V.H., Marx, B.D., Coronado-Molina, C., Ewe, S.M.L., 2011. Patterns of Root Dynamics in Mangrove Forests Along

Environmental Gradients in the Florida Coastal Everglades, USA. Ecosystems 14, 1178–1195.

Chmura, G.L., 2013. What do we need to assess the sustainability of the tidal salt marsh carbon sink? Ocean Coast. Manag. 83, 25–31.

Chmura, G.L., Anisfeld, S.C., Cahoon, D.R., Lynch, J.C., 2003. Global carbon sequestration in tidal, saline wetland soils. Global Biogeochem. Cycles 17, 1–12.

Choi, Y., Wang, Y., Hsieh, Y.P., Robinson, L., 2001. Vegetation succession and carbon sequestration in a coastal wetland in northwest Florida: Evidence from carbon isotopes. Global Biogeochem. Cycles 15, 311–319.

Comley, B.W.T., McGuinness, K.A., 2005. Above and belowground biomass, and allometry, of four common northern Australian mangroves. Aust. J. Bot. 53, 431–436.

Cormier, N., Twilley, R.R., Ewel, K.C., Krauss, K.W., 2015. Fine root productivity varies along nitrogen and phosphorus gradients in high-rainfall mangrove forests of Micronesia. Hydrobiologia 750, 69–87.

Donato, D.C., Kauffman, J.B., Murdiyarso, D., Kurnianto, S., Stidham, M., Kanninen, M., 2011. Mangroves among the most carbon - rich forests in the tropics. Nat. Geosci. 4, 293–297.

Doughty, C.L., Langley, J.A., Walker, W.S., Feller, I.C., Schaub, R., Chapman, S.K., 2016. Mangrove Range Expansion Rapidly Increases Coastal Wetland Carbon Storage. Estuaries and Coasts 39, 385–396.

Duarte, C.M., Losada, I.J., Hendriks, I.E., Mazarrasa, I., Marbà, N., 2013. The role of coastal plant communities for climate change mitigation and adaptation. Nat. Clim. Chang. 3, 961–968.

Duarte, C.M., Middelburg, J.J., Caraco, N., 2005. Major role of marine vegetation on the oceanic carbon cycle. Biogeosciences 2, 1–8.

Fink, D., Hotchkis, M., Hua, Q., Jacobsen, G., Smith, A.M., Zoppi, U., Child, D., Mifsud, C., Gaast, H. Van Der, Williams, A., Williams, M., 2004. The ANTARES AMS facility at ANSTO. Nucl. Instruments Methods Phys. Res. B Beam Interact. with Mater. Atoms 223–224, 109–115.

Greiner, J.T., McGlathery, K.J., Gunnell, J., McKee, B.A., 2013. Seagrass Restoration

Enhances "Blue Carbon" Sequestration in Coastal Waters. PLoS One 8, 1–8.

Grimsditch, G., Alder, J., Nakamura, T., Kenchington, R., Tamelander, J., 2013. The blue carbon special edition – Introduction and overview. Ocean Coast. Manag. 83, 1–4.

Hayes, M.A., Jesse, A., Tabet, B., Reef, R., Keuskamp, J., Lovelock, C.E., 2017. The contrasting effects of nutrient enrichment on growth, biomass allocation and decomposition of plant tissue in coastal wetlands. Plant Soil 416, 193–204.

Howard, J., Hoyt, S., Isensee, K., Pidgeon, E., Telszewski, M., 2014. Coastal Blue Carbon: Methods for Assessing Carbon Stocks and Emissions Factors in Mangroves, Tidal Salt Marshes, and Seagrass Meadows. Intergov. Oceanogr. Comm. UNESCO, Int. Union Conserv. Nature. Arlington, Virginia, USA.

Howe, A.J., Rodríguez, J.F., Saco, P.M., 2009. Surface evolution and carbon sequestration in disturbed and undisturbed wetland soils of the Hunter estuary, southeast Australia. Estuar. Coast. Shelf Sci. 84, 75–83.

Hua, Q., Jacobsen, G.E., Zoppi, U., Lawson, E.M., Williams, A.A., Smith, A.M., McGann, M.J., 2001. Progress in radiocarbon target preparation at the ANTARES AMS centre. Radiocarbon 43, 275–282.

Jardine, S.., Siikamäki, J.., 2014. A global predictive model of carbon in mangrove soils. Environ. Res. Lett. 9, 1–9.

Jennerjahn, T.C., Ittekkot, V., 2002. Relevance of mangroves for the production and deposition of organic matter along tropical continental margins. Naturwissenschaften 89, 23–30.

Kauffman, J.B., Heider, C., Norfolk, J., Payton, F., 2014. Carbon stocks of intact mangroves and carbon emissions arising from their conversion in the Dominican Republic. Ecol. Appl. 24, 518–527.

Kelleway, J.J., Mazumder, D., Baldock, J.A., Saintilan, N., 2018. Carbon isotope fractionation in the mangrove Avicennia marina has implications for food web and blue carbon research. Estuar. Coast. Shelf Sci. 205, 68–74.

Kelleway, J.J., Saintilan, N., Macreadie, P.I., Skilbeck, C.G., Zawadzki, A., Ralph, P.J., 2016a. Seventy years of continuous encroachment substantially increases "blue carbon" capacity as mangroves replace intertidal salt marshes. Glob. Chang. Biol.

22, 1097–1109.

Kelleway, J.J., Saintilan, N., Macreadie, P.I., Ralph, P.J., 2016b. Sedimentary Factors are Key Predictors of Carbon Storage in SE Australian Saltmarshes. Ecosystems 19, 865–880.

Kirui, K.B., Kairo, J.G., Bosire, J., Viergever, K.M., Rudra, S., Huxham, M., Briers, R.A., 2013. Mapping of mangrove forest land cover change along the Kenya coastline using Landsat imagery. Ocean Coast. Manag. 83, 19–24.

Komiyama, A., Ogino, K., Aksornkoae, S., Sabhasri, S., 1987. Root biomass of a mangrove forest in southern Thailand. 1. Estimation by the trench method and the zonal structure of root biomass. J. Trop. Ecol. 3, 97–108.

Komiyama, A., Ong, J.E., Poungparn, S., 2008. Allometry, biomass, and productivity of mangrove forests: A review. Aquat. Bot. 89, 128-137.

Kristensen, E., Bouillon, S., Dittmar, T., Marchan, C., 2008. Organic carbon dynamics in mangrove ecosystems: A review. Aquat. Bot. 89, 201–219.

Lang'at, J.K.S., Kirui, B.K.Y., Skov, M.W., Kairo, J.G., Mencuccini, M., Huxham, M., 2013. Species mixing boosts root yield in mangrove trees. Oecologia 172, 271–278.

Liu, H., Ren, H., Hui, D., Wang, W., Liao, B., Cao, Q., 2014. Carbon stocks and potential carbon storage in the mangrove forests of China. J. Environ. Manage. 133, 86–93.

Liu, X., Xiong, Y., Liao, B., 2017. Relative contributions of leaf litter and fine roots to soil organic matter accumulation in mangrove forests. Plant Soil 421, 493–503.

Lovelock, C.E., Cahoon, D.R., Friess, D.A., Guntenspergen, G.R., Krauss, K.W., Reef, R., Rogers, K., Saunders, M.L., Sidik, F., Swales, A., Saintilan, N., Thuyen, L.X., Triet, T., 2015. The vulnerability of Indo-Pacific mangrove forests to sea-level rise. Nature 526, 559-U217.

Lovelock, C.E., Fernanda Adame, M., Bennion, V., Hayes, M., Reef, R., Santini, N.S., 2013. Contemporary Rates of Carbon Sequestration Through Vertical Accretion of Sediments in Mangrove Forests and Saltmarshes of South East Queensland, Australia. Estuaries and Coasts 37, 763–771.

Lunstrum, A., Chen, L., 2014. Soil carbon stocks and accumulation in young mangrove forests. Soil Biol. Biochem. 75, 223–232.

Maher, D., Santos, I., Schulz, K., Call, M., Jacobsen, G., Sanders, C., 2017. Blue carbon oxidation revealed by radiogenic and stable isotopes in a mangrove system. Geophys. Res. Lett. 44, 4889–4896.

Marbà, N., Arias-Ortiz, A., Masqué, P., Kendrick, G.A., Mazarrasa, I., Bastyan, G.R., Garcia-Orellana, J., Duarte, C.M., 2015. Impact of seagrass loss and subsequent revegetation on carbon sequestration and stocks. J. Ecol. 103, 296–302.

Marchand, C., 2017. Soil carbon stocks and burial rates along a mangrove forest chronosequence (French Guiana). For. Ecol. Manage. 384, 92–99.

Marland, G., Mccarl, B.A., Schneider, U.W.E., 2001. Soil Carbon: Policy and Economics. Clim. Change 51, 101–117.

Mcleod, E., Chmura, G.L., Bouillon, S., Salm, R., Björk, M., Duarte, C.M., Lovelock, C.E., Schlesinger, W.H., Silliman, B.R., 2011. A blueprint for blue carbon: Toward an improved understanding of the role of vegetated coastal habitats in sequestering CO2. Front. Ecol. Environ. 9, 552–560.

Naidoo, G., 2009. Differential effects of nitrogen and phosphorus enrichment on growth of dwarf Avicennia marina mangroves. Aquat. Bot. 90, 184–190.

Njana, M.A., Eid, T., Zahabu, E., Malimbwi, R., 2015. Procedures for quantification of belowground biomass of three mangrove tree species. Wetl. Ecol. Manag. 23, 749–764.

Osland, M.J., Spivak, A.C., Nestlerode, J.A., Lessmann, J.M., Almario, A.E., Heitmuller, P.T., Russell, M.J., Krauss, K.W., Alvarez, F., Dantin, D.D., Harvey, J.E., From, A.S., Cormier, N., Stagg, C.L., 2012. Ecosystem Development After Mangrove Wetland Creation: Plant–Soil Change Across a 20-Year Chronosequence. Ecosystems 15, 848–866.

Ouyang, X., Lee, S.Y., 2014. Updated estimates of carbon accumulation rates in coastal marsh sediments. Biogeosciences 11, 5057–5071.

Owers, C.J., Rogers, K., Woodroffe, C.D., 2018. Spatial variation of aboveground carbon storage in temperate coastal wetlands. Estuar. Coast. Shelf Sci. 210, 55–67.

Pendleton, L., Donato, D.C., Murray, B.C., Crooks, S., Jenkins, W.A., Sifleet, S., Craft, C., Fourqurean, J.W., Kauffman, J.B., Marbà, N., Megonigal, P., Pidgeon, E., Herr, D., Gordon, D., Baldera, A., 2012. Estimating Global "Blue Carbon" Emissions from

Conversion and Degradation of Vegetated Coastal Ecosystems. PLoS One 7, 1–7.

Reef, R., Slot, M., Motro, U., Motro, M., Motro, Y., Adame, M.F., Garcia, M., Arande, J., Lovelock, C.E., Winter, K., 2016. The effects of CO_2 and nutrient fertilisation on the growth and temperature response of the mangrove Avicennia germinans. Photosynth. Res. 129, 159–170.

Reef, R., Winter, K., Morales, J., Adame, M., Reef, D.L., 2015. The effect of atmospheric carbon dioxide concentrations on the performance of the mangrove Avicennia germinans over a range of salinities. Physiol. Plant. 154, 358–368.

Rodrigues, D.P., Hamacher, C., Estrada, G.C.D., Soares, M.L.G., 2015. Variability of carbon content in mangrove species: Effect of species, compartments and tidal frequency. Aquat. Bot. 120, 346–351.

Rogers, K., Boon, P.I., Branigan, S., Duke, N.C., Field, C.D., Fitzsimons, J.A., Kirkman, H., Mackenzie, J.R., Saintilan, N., 2016. The state of legislation and policy protecting Australia's mangrove and salt marsh and their ecosystem services. Mar. Policy. 72, 139–155.

Rovai, A.S., Twilley, R.R., Castañeda-moya, E., Riul, P., Cifuentes-jara, M., Manrow-villalobos, M., Horta, P.A., Simonassi, J.C., Fonseca, A.L., Pagliosa, P.R., 2018. Global controls on carbon storage in mangrove soils. Nat. Clim. Chang. 8, 534–538.

Saintilan, N., 1989. Mangrove distribution in the Hawkesbury River. Honours thesis, University of Sydney, Sydney, NSW.

Saintilan, N., 1995. Variation in mangrove community characteristics within two east-coast Australian estuaries. PhD thesis, University of Sydney, Sydney, NSW.

Saintilan, N., 1997. Above and belowground biomasses of two species of mangrove on the Hawkesbury River estuary, New South Wales. Mar. Freshw. Res. 48, 147–152.

Saintilan, N., Hashimoto, T.R., 1999. Mangrove-saltmarsh dynamics on a bay-head delta in the Hawkesbury River estuary , New South Wales , Australia. Hydrobiologia. 413, 95–102.

Saintilan, N., Rogers, K., 2015. Woody plant encroachment of grasslands: a comparison of terrestrial and wetland settings. New Phytol. 205, 1062–1070.

Saintilan, N., Rogers, K., Mazumder, D., Woodroffe, C., 2013. Allochthonous and autochthonous contributions to carbon accumulation and carbon store in

southeastern Australian coastal wetlands. Estuar. Coast. Shelf Sci. 128, 84–92.

Saintilan, N., Williams, R., 1999. Mangrove transgression into saltmarsh environments in south-east Australia 8, 117–124.

Saintilan, N., Wilson, N.C., Rogers, K., Rajkaran, A., Krauss, K.W., 2014. Mangrove expansion and salt marsh decline at mangrove poleward limits. Glob. Chang. Biol. 20, 147–157.

Schlacher, T.A., Connolly, R.M., 2014. Effects of acid treatment on carbon and nitrogen stable isotope ratios in ecological samples: a review and synthesis. Methods Ecol. Evol. 5, 541–550.

Tamooh, F., Huxham, M., Karachi, M., Mencuccini, M., Kairo, J.G., Kirui, B., 2008. Belowground root yield and distribution in natural and replanted mangrove forests at Gazi bay, Kenya. For. Ecol. Manage. 256, 1290–1297.

Thomas, S., 2014. Blue carbon: Knowledge gaps, critical issues, and novel approaches. Ecol. Econ. 107, 22–38.

Trevathan-Tackett, S.M., Kelleway, J., Macreadie, P.I., Beardall, J., Ralph, P., Bellgrove, A., 2015. Comparison of marine macrophytes for their contributions to blue carbon sequestration. Ecology 96, 3043–3057.

Twilley, R.R., Chen, R., Hargis, T., 1992. Carbon sinks in mangroves and their implications to carbon budget of tropical coastal ecosystems. Water, Air Soil Pollut. 64, 265–288.

Twilley, R.R., Rovai, A.S., Riul, P., 2018. Coastal morphology explains global blue carbon distributions. Front. Ecol. Environ. 16, 1–6.

Walcker, R., Gandois, L., Proisy, C., Corenblit, D., Christophe, M., Raghab, L., Franc, R., 2018. Control of "blue carbon" storage by mangrove ageing: Evidence from a 66-year chronosequence in French Guiana. Glob. Chang. Biol. 24, 2325–2338.

Webb, E.L., Friess, D. a, Krauss, K.W., Cahoon, D.R., Guntenspergen, G.R., Phelps, J., 2013. A global standard for monitoring coastal wetland vulnerability to accelerated sea-level rise. Nat. Clim. Chang. 3, 458–465.